

Relaxation of electronic excitations in Kr-2(+) ions in cold krypton plasma

Cyril van de Steen, Malika Benhenni, René Kalus, Rajko Ćosić, Florent X. Gadéa, Mohammed Yousfi

▶ **To cite this version:**

Cyril van de Steen, Malika Benhenni, René Kalus, Rajko Ćosić, Florent X. Gadéa, et al.. Relaxation of electronic excitations in Kr-2(+) ions in cold krypton plasma. Plasma Sources Science and Technology, 2020, 29 (2), pp.025004. 10.1088/1361-6595/ab5f42 . hal-02512355

HAL Id: hal-02512355
https://hal.science/hal-02512355

Submitted on 14 Dec 2020

HAL is a multi-disciplinary open access archive for the deposit and dissemination of scientific research documents, whether they are published or not. The documents may come from teaching and research institutions in France or abroad, or from public or private research centers.

L'archive ouverte pluridisciplinaire **HAL**, est destinée au dépôt et à la diffusion de documents scientifiques de niveau recherche, publiés ou non, émanant des établissements d'enseignement et de recherche français ou étrangers, des laboratoires publics ou privés.

APS/123-QED

Relaxation of electronic excitations in Kr_2^+ ions in cold krypton plasma.

Cyril Van de Steen,[1,2,*] Malika Benhenni,[2,†] René Kalus,[1,‡]
Rajko Ćosić,[1,3] Florent Xavier Gadéa,[4] and Mohammed Yousfi[2]

[1]*IT4Innovations, VSB - Technical University of Ostrava, 17. listopadu 2172/15, 708 00 Ostrava-Poruba, Czech Republic.*

[2]*Laboratoire Plasma et Conversion d'Energie, LAPLACE & UMR5213 du CNRS, Université de Toulouse III Paul Sabatier, 118 route de Narbonne, 31062 Toulouse Cedex, France.*

[3]*Department of Applied Mathematics, Faculty of Electrical Engineering and Computer Science, VSB - Technical University of Ostrava, 17. listopadu 2172/15, 708 00 Ostrava-Poruba, Czech Republic.*

[4]*Laboratoire de Chimie et de Physique Quantiques, IRSAMC & UMR5626 du CNRS, Université de Toulouse III Paul Sabatier, 31062 Toulouse Cedex 09, France.*

(Dated: November 20, 2019)

Abstract

Reaction rate constants have been calculated for electronic transitions in Kr_2^+ ions and for their decay as induced by collisions with krypton atoms and/or spontaneous radiation processes. The rate constants have then been used in a series of modelings of electronic relaxation in the ions in cold krypton plasmas with the main focus on relaxation times and final states. It has been shown that the collision-induced (non-radiative) relaxation is much faster than the radiative one and completely dominates with typical relaxation times ranging between nanoseconds and microseconds. The relaxation always ends up in the Kr_2^+ electronic ground state, high electronic excitations survive for longer times than lower excitations due to spin-orbit coupling effects.

PACS numbers: 52.20.-j 52.20.Hv 34.50.-s

*Electronic address: cyril.vds@gmail.com

[†]Electronic address: malika.benhenni@laplace.univ-tlse.fr
[‡]Electronic address: rene.kalus@vsb.cz

I. INTRODUCTION

Cold rare-gas plasmas have recently received a considerable attention raised by a promising potential in various applications. Among others, biomedicine [1–3] and spacecraft propulsion [4, 5] may serve as the most pronounced examples. In complement to the experimental research, numerical modeling plays an important role in plasma physics, mainly because they are able to provide a deep insight into phenomena and processes not usually accessible by experiments. It is particularly important for rare-gas plasmas since various aspects of their physics are to be deeply understood in order to control and tailor their properties important for their efficient applications. For example, the formation of active species (radicals, excited species, charged particles etc.) and the basic data on their reactivity and transport are of particular importance in fluid dynamics modelings of cold rare-gas plasmas and tailoring their characteristics.

Ions of various kinds have a major effect on the magnitude of the space charge electric field and, in turn, are determinant or even decisive for the formation and the densities of many other active species in cold plasmas. In rare-gas plasmas, in particular, atomic ions would primarily be expected to be by far the most abundant ones and, thus, to play the most important role in influencing plasmas properties. However, it was shown a long time ago [6–8] that molecular ions of small sizes, namely, dimers and trimers, also play a significant role, which is a clear consequence of their rather strong binding. Specifically, the krypton dimer ion, Kr_2^+, may serve as a good example with its binding being of almost chemical strength ($D_0 \approx 1.15\,\mathrm{eV}$) [9, 10]. This stands in a clear contrast to the neutral krypton dimer, Kr_2, the binding energy of which is too small ($D_0 \approx 0.016\,\mathrm{eV}$ [11]) for the Kr_2 molecule to survive, at ambient conditions, at a non-negligible amount [12].

The krypton dimer ion cannot thus arise from a direct ionization of its neutral precursor and alternative mechanisms were also proposed [6]: a) the *three-body recombination*,

$$\mathrm{Rg}^+ + \mathrm{Rg} + \mathrm{Rg} \rightarrow \mathrm{Rg}_2^+ + \mathrm{Rg} \tag{1}$$

and b) the *associative ionization* (the asterisk on the left-hand-side denotes electronic excitation),

$$\mathrm{Rg}^* + \mathrm{Rg} \rightarrow \mathrm{Rg}_2^+ + \mathrm{e}^-, \tag{2}$$

the latter being also called the *Hornbeck-Molnar process*. Since electronically excited

monomers participate on the reactant side not only in the reaction given by Eq. (2), but also in the three-body recombination process [13], electronically excited products (dimer ions) are highly probably to be produced and the initial electronic excitation is only afterwards relaxed. However, the processes of such relaxation cannot be easily monitored experimentally and theoretical modeling is thus strongly needed. The relaxation of electronic excitations in atomic and molecular ions colliding with atoms has also been studied elsewhere [14–18], however the context of cold atoms physics is quite different from the cold plasma one, and mainly charge transfer processes were investigated in these works.

In two preceding papers [19, 20] we have investigated transport properties of the krypton dimer ion in the electronic ground state [19] and low-lying excited states [20]. Since the results we obtained are compatible for both ground-state and excited-state dimers with available experimental data [6], both types of the Kr_2^+ dimer may be present in experimental populations. However, the experimental data do not allow to make an (at least rough) quantitative estimate of how various electronic excitations are populated in Kr_2^+ under typical experimental conditions.

The abundances of particular electronic states are basically influenced by two factors: a) the way how the Kr_2^+ ions are formed and b) how the nascent population of electronic excitations is afterward relaxed. In the present work, we focus on the latter issue and provide an introductory study of processes responsible for the relaxation of the nascent electronic excitation in krypton dimer ions. It is noteworthy that both spontaneous radiative transitions as well as non-radiative, collision-induced processes may in principle play a role and are, thus, considered.

The results reported in the present paper are mostly based on our preceding dynamical calculations on the Kr_2^+/Kr collisions [19, 20], the outputs of which have been analyzed in a more detailed way here, however, which has enabled detection of particular electronic states on the output. This has allowed to assess all the parameters governing the relaxation of the initial electronic excitation in the Kr_2^+ ion, namely, effective collision cross-sections of state-to-state transitions and related rate constants. The calculated rate constants have then been used, together with rate constants of radiative transitions calculated here using a semiclassical approach (see Sec. II B 2) and rate constants of collision-induced dimer ion disappearance reported in preceding studies [19, 20], in kinetic modelings of electronic relaxation in Kr_2^+.

It should be noted that the considered reaction rate constants may in general depend on the initial rotational-vibrational excitation of the ionic dimer. Therefore, they have to be properly averaged over the rotational-vibrational states following, e.g., thermal distributions. However, such a full calculation considering both the (six) electronic states and (dozens of) rotational-vibrational states of the ionic dimer is clearly beyond the scope of the present work. For simplicity and to avoid calculations of impracticable extent, only the rotational-vibrational ground state, $[j = 0, v = 0]$, has been considered for each Kr_2^+ electronic state. Despite this, we believe that the results obtained may still provide qualitatively sound, or even semi-quantitative estimates of the efficiency of the electronic relaxation in Kr_2^+ and the relevance of particular electronic states in Kr_2^+ populations in cold krypton plasmas.

The present paper is organized as follows. First, methodological approaches and computations are reviewed in Sec. II. Specifically, processes considered in the present model of the electronic relaxation in Kr_2^+ are summarized in Subsec. II A, the methods of the calculation of needed rate constants are discussed in Subsec. II B, and, finally, kinetic equations governing the electronic relaxation in Kr_2^+ are introduced and methods for their solution are described in Subsec. II C. Then, main results are presented and discussed in Sec. III, with calculated rate constants summarized in Subsec. III A and typical relaxation evolutions of selected nascent populations of electronic excitations in Kr_2^+ discussed in Subsec. III B. Finally, conclusive remarks and outlooks are provided in Sec. IV.

II. METHODS AND COMPUTATIONS

A. Processes

The following low-lying electronic states of the Kr_2^+ ion and transitions among them have been considered, the $I(1/2)_u$ ground state, excited states asymptotically correlating to the fine-structure ground state ($^2P_{3/2}$) of the atomic ion, $I(3/2)_g$, $I(3/2)_u$ and $I(1/2)_g$ (group I states), and excited states asymptotically correlating to the Kr^+ fine-structure excited state ($^2P_{1/2}$), $II(1/2)_u$ and $II(1/2)_g$ (group II states). A graphical summary of them is provided in Fig. 1.

Two kinds of transition processes are considered in the present work, (non-radiative) *collision-induced transitions* and *spontaneous radiative transitions* in free ionic dimers. As

discussed elsewhere [21], radiative processes do not play an important role during the collision compared to non-radiative processes and are thus neglected here [22]. Since, in addition, the probability of non-radiative transitions is very small in free Kr_2^+ ions (exactly zero if the spin-orbit coupling is neglected), the non-radiative free-flight transitions are neither considered here.

Both collision-induced processes and spontaneous radiative processes may result either in an electronic transition in the dimer ion or in the dimer ion disappearance, the latter mainly due to dimer dissociation [23] and, consequently, the following processes have to be considered (small Greek letters represent particular electronic states of the dimer [24]):
collision-induced inter-state transition (cIST),

$$Kr_2^+(\alpha) + Kr \rightarrow Kr_2^+(\beta) + Kr, \tag{3}$$

collision-induced dimer ion disappearance (cDID),

$$Kr_2^+(\alpha) + Kr \rightarrow Kr^+ + 2Kr/Kr_2, \tag{4}$$

radiative inter-state transition (rIST),

$$Kr_2^+(\alpha) \rightarrow Kr_2^+(\beta) + h\nu, \tag{5}$$

and *radiative dimer dissociation* (rDD)

$$Kr_2^+(\alpha) \rightarrow Kr^+ + Kr + h\nu. \tag{6}$$

Note that the two latter processes are used to discriminate between radiative transitions resulting to a stabilized dimer on the output, Eq. (5), and transitions from a bound rotational-vibrational state to a continuum state leading to dimer dissociation, Eq. (6).

All the processes given by Eqs. (3)–(6) are considered in the present work with related rate constants denoted as $k^{(3)}_{\alpha\beta}$, $k^{(4)}_{\alpha}$, $k^{(5)}_{\alpha\beta}$, and $k^{(6)}_{\alpha}$, respectively, where the upper index indicates the number of the equation describing each particular process.

B. Reaction rate constants

1. *Rate constants of collision-induced processes*

The present calculations related to the collision-induced processes, Eqs. (3) and (4), heavily rely on the data reported in the preceding studies on the Kr_2^+/Kr collisions [19,

20]. To summarize, let us recall that, in those studies, we calculated bunches of Kr_2^+/Kr (quasiclassical) collision trajectories for the dimer ion being, prior to a collision, either in its electronic ground state [$I(1/2)_u$] or in one of the five lowest excited states [$I(3/2)_g$, $I(3/2)_u$, $I(1/2)_g$, $II(1/2)_u$, and $II(1/2)_g$]. For each electronic state, a broad range of (center-of-mass) collision energies was considered (between $E_{coll} = 0.01\,eV$ and $E_{coll} = 100\,eV$), and, for each collision energy, a sufficiently large number of impact-parameter values were included and sampled between $b = 0$ and $b = b_{max}$ ($b_{max} = 10{-}30\,Å$, depending on the electronic state and collision energy) with a step of $\Delta b = 0.1\,Å$. Altogether 528 trajectories were integrated numerically for each value of the impact-parameter. They started from a sample of Kr_2^+/Kr initial conditions imitating experimental conditions and covering various (isotropic) orientations of the dimer ion in space and various phases of its rotational-vibrational motion [25]. Note also that the forces due to the external electric field are completely negligible compared to inter-atomic interactions and, consequently, the external electric field has not been considered in trajectory calculations.

Totally, 50,000 to 150,000 trajectories were evaluated for each collision energy and electronic state, and subsequently were used to evaluate effective cross-sections of particular collision channels. Following the conclusions of an immediately preceding study [20], electronic potentials of Ref. 9 (referred therein as model B) have been used in calculations on the Kr_2^+ ion starting from the electronic ground state and the potentials of Ref. 10 (model A) have been employed for electronically excited dimers.

The rate constants of cDID processes, Eq. (4), were calculated in the two preceding studies [19, 20] and are used here without any additional modification.

Alike, most of the data needed to calculate the rate constants of the cIST processes, Eq. (3), were reported in the two preceding studies and, here, they have been re-analyzed in a more detailed way. More specifically, final electronic states of the dimer [denoted by index β in Eq. (3)] have been considered explicitly for each collision trajectory and their relative abundances have been calculated for each particular value of the impact-parameter (and for each initial electronic state, α, of the dimer ion). If we denote these abundances as $x_{\alpha\beta}(b)$, then the effective cross-sections of processes given by Eq. (3) can be calculated from

$$\sigma^{(3)}_{\alpha\beta} = \int_0^{b_{max}} x_{\alpha\beta}(b)\; 2\pi b\; \mathrm{d}b. \tag{7}$$

Corresponding rate constants have then been obtained from these cross-sections (and

momentum-transfer cross-sections of $Kr_2^+(\alpha)$/Kr collisions reported in Refs. 19 and 20) via a series of Monte Carlo simulations [26] described in detail, e.g., in Sec. 2.3 of Ref. 19. Briefly, a sufficiently large number of trajectories of the dimer ion (prepared in a specific electronic state and propagated under the action of a uniform electric field) are generated with collisions evoked with probabilities given by the pre-calculated effective cross-sections. Since weakly ionized gas is assumed, only collisions with neutral atoms are considered [27]. The propagation of each ion takes place until the latter disappears (dissociates) and/or time limits indicating that the cathode has been reached or the prefixed simulation time has been elapsed are exceeded. The reaction rate constant of a particular cIST process is then obtained from (see, e.g., Sec. 2.3 of Ref. 19)

$$k_{\alpha\beta}^{(3)} = \frac{\left\langle \nu_{\alpha\beta}^{(3)} \right\rangle}{N}, \tag{8}$$

where N denotes particle density of the gas and $\left\langle \nu_{\alpha\beta}^{(3)} \right\rangle$ is the average frequency of collisions leading to an $\alpha \to \beta$ transition in the colliding dimer ion.

2. Rate constants of spontaneous radiative processes

The processes resulting from radiative transitions in the Kr_2^+ ion basically consist of two steps. Firstly, an electronic transition takes place (accompanied by the emission of a photon) and, secondly, the dimer either survives or dissociates depending on whether the transition yields a bound rotational-vibrational state or a continuum state. Alike for collision-induced processes, the effect of the external electric field is completely negligible and it need not be considered for radiative processes. Moreover, since the electronic transition is much slower than the following dissociation of the dimer (if any), the rate of the overall process is completely governed by the rate of the former process. The rate constant of a radiative transition going from state α to state β ($\Gamma_{\alpha\beta}$) is given, for a particular nuclear configuration ($\mathbf{R}$), from Fermi's golden rule [28],

$$\Gamma_{\alpha\beta}(\mathbf{R}) = \frac{1}{3\pi\varepsilon_0\hbar^4c^3}\left[E_\alpha(\mathbf{R}) - E_\beta(\mathbf{R})\right]^3 \left|\mu_{\alpha\beta}(\mathbf{R})\right|^2, \tag{9}$$

where ε_0, $\hbar$, and c are the vacuum permittivity, the (reduced) Planck constant, and the vacuum light velocity, respectively, E_α and E_β are (adiabatic) electronic energies before and after the transition, respectively, and $\mu_{\alpha\beta}$ is the transition dipole moment between states α

and β, both evaluated in nuclear geometry $\mathbf{R}$. For flexible molecules, the values obtained from Eq. (9) have to be averaged over a representative set of molecular geometries. In the case of the Kr_2^+ dimer, it means that averaging over properly sampled inter-atomic distances has to be done. For example, sampling from (the square of) the nuclear wave function corresponding to a specific rotational-vibrational state of the dimer ($[j = 0, v = 0]$ in this work) can be used.

Only specific spontaneous radiative transitions are allowed in the krypton dimer ion if a first-order (dipole) approximation adopted in Eq. (9) is used:

$$\begin{aligned} &\mathrm{II}(1/2)_\mathrm{g} \rightarrow \mathrm{II}(1/2)_\mathrm{u} \quad [\alpha = 6 \rightarrow \beta = 5], \\ &\mathrm{II}(1/2)_\mathrm{g} \rightarrow \mathrm{I}(1/2)_\mathrm{u} \quad [\alpha = 6 \rightarrow \beta = 1], \\ &\mathrm{I}(3/2)_\mathrm{u} \rightarrow \mathrm{I}(3/2)_\mathrm{g} \quad [\alpha = 3 \rightarrow \beta = 2], \end{aligned} \tag{10}$$

$$\mathrm{I}(1/2)_\mathrm{g} \rightarrow \mathrm{I}(1/2)_\mathrm{u} \quad [\alpha = 4 \rightarrow \beta = 1], \tag{11}$$

and

$$\mathrm{II}(1/2)_\mathrm{u} \rightarrow \mathrm{I}(1/2)_\mathrm{g} \quad [\alpha = 5 \rightarrow \beta = 4]. \tag{12}$$

Since the transitions given by Eq. (10) end up in a bound (though often excited) rotational-vibrational state on the final electronic potential energy curve, they are hereafter treated as rIST processes of Eq. (5). The transition given by Eq. (12), on the other hand, ends always in a continuum state of the $\mathrm{I}(1/2)_\mathrm{g}$ potential and is thus treated as an rDD process given by Eq. (6). Finally, the process given by Eq. (11) should mostly lead to a bound electronically ground-state dimer, but in an extremely highly excited rotational-vibrational state, lying just below the dissociation limit. For this reason, the process of Eq. (11) is assumed to be an rDD [Eq. (6)]. As a consequence, the rate constants of the spontaneous emission processes have been set as follows (brackets indicate averaging over Kr_2^+ inter-nuclear distances): $k_{65}^{(5)} = \langle\Gamma_{65}\rangle$, $k_{61}^{(5)} = \langle\Gamma_{61}\rangle$, $k_{32}^{(5)} = \langle\Gamma_{32}\rangle$, $k_{4}^{(6)} = \langle\Gamma_{41}\rangle$, and $k_{5}^{(6)} = \langle\Gamma_{54}\rangle$. The remaining radiative rate constants are equal to zero.

C. Modeling of kinetics of Kr_2^+ inter-state transitions and decay

Though Eqs. (3)–(6) do not represent a complete description of processes one can anticipate in cold krypton plasma, e.g., reactions leading to the formation of the Kr_2^+ ion are

not included, they may provide a qualitatively sound picture of how initial electronic excitations are relaxed in a population of Kr_2^+ ions. Corresponding time evolution is governed by the following kinetic equations [n_α denotes the particle density of the $Kr_2^+(\alpha)$ ion]:

$$\frac{\mathrm{d}n_\alpha}{\mathrm{d}t} = -K_\alpha n_\alpha + \sum_{\beta\neq\alpha} K_{\beta\alpha} n_\beta, \tag{13}$$

where

$$\begin{aligned} K_\alpha &= \left[\sum_{\beta\neq\alpha} k_{\alpha\beta}^{(3)} + k_\alpha^{(4)}\right] n_\mathrm{g} + \sum_{\beta\neq\alpha} k_{\alpha\beta}^{(5)} + k_\alpha^{(6)}, \\ K_{\beta\alpha} &= k_{\beta\alpha}^{(3)} n_\mathrm{g} + k_{\beta\alpha}^{(5)}. \end{aligned} \tag{14}$$

In Eqs. (14), n_g denotes the particle density of the carrier gas. This density is considered constant and is obtained from the gas pressure (P) and temperature (T) calculated within the ideal-gas approximation, $n_\mathrm{g} = P/(k_\mathrm{B}T)$.

Eq. (13) can be rewritten in a compact matrix form,

$$\frac{\mathrm{d}\mathbf{n}}{\mathrm{d}t} = \mathbf{A}\cdot\mathbf{n}, \tag{15}$$

where $\mathbf{n}$ is a six dimensional column vector of $Kr_2^+(\alpha)$ concentrations, $\mathbf{A}$ is a 6×6 matrix corresponding to the constant coefficients of the right-hand side of Eq. (13), and the dot denotes matrix multiplication. Using this compact form of the kinetics equations, their (unique) solution corresponding to an initial condition $\mathbf{n}(0) = \mathbf{n}_0$ can be expressed as

$$\mathbf{n}(t) = \exp(\mathbf{A}t)\cdot\mathbf{n}_0. \tag{16}$$

A symplectic integrator based on a second-order approximation of the matrix exponential, $\exp(\mathbf{A}\Delta t) \approx \mathbf{1} + \mathbf{A}\Delta t + 1/2(\mathbf{A}\Delta t)^2$, has been employed to evaluate this solution numerically.

III. RESULTS AND DISCUSSIONS

A. Reaction rate constants

1. *Dimer ion disappearance rate constants*

As mentioned above, the *collision-induced dimer ion disappearance* (cDID) rate constants were reported for the Kr_2^+ ion in two immediately preceding studies [19, 20] and the reader is

referred therein for necessary details. For completeness, they are also summarized in a form appropriate for the present analysis [29] in Fig. 2.

Rate constants of *radiative dimer dissociation* (rDD) processes [Eqs. (11) and (12)] calculated in this work are also added in Fig. 2 for comparison. However, since the rDD rate constants are, at ambient conditions ($T = 300\,\mathrm{K}$ and $P = 760\,\mathrm{Torr}$), about 2–4 orders of magnitudes smaller than respective cDID rate constants (see also Table I), it seems that the radiative dissociation of the electronically excited Kr_2^+ ions plays only a negligible role at room temperature and atmospheric pressure. Interestingly, this holds even if weak external fields (resulting in low Kr_2^+/Kr collision energies) are considered.

2. Inter-state transition rate constants

The inter-state transition rate constants, as calculated for rotationally-vibrationally ground-state Kr_2^+ dimers, are summarized in Fig. 3. Both collision-induced inter-state transitions (cIST) as well as radiative transitions (rIST) are considered (for the latter see also Table I). A couple of important observations are clear from the figure.

Firstly, the radiative (rIST) processes are either significantly less efficient than the collision-induced (cIST) processes or, at the utmost, comparable to them. But, the latter holds only when collision-induced transitions themselves are unimportant. It thus seems that the radiative transitions will play a negligible role for inter-state transitions [30] as well as for the dimer disappearance.

Secondly, the rate constants of transitions from group I to group II are either zero or by at least two orders of magnitude smaller than the rate constants of transitions occurring among states of group I. The group I to group II transitions are thus expected to play only a marginal role and, as expected [20], the electronic relaxation of group I states is almost quasiadiabatic, i.e., confined to the group I manifold.

Thirdly, the situation is somewhat more involved for intergroup transitions. While the transitions starting from the $\mathrm{II}(1/2)_\mathrm{g}$ state dominantly go to the $\mathrm{II}(1/2)_\mathrm{u}$ state, i.e., they are confined within group II and are, thus, quasiadiabatic, the lower of the group II states, $\mathrm{II}(1/2)_\mathrm{u}$, may undergo collision-induced transitions to both the other state of group II, $\mathrm{II}(1/2)_\mathrm{g}$, and the states of group I (mainly the ground state). This particularly holds if a weak electric field is applied ($E/N \lesssim 30\,\mathrm{Td}$) where the two kinds of transitions are of

a more or less equal probability. As a consequence, the $\mathrm{II}(1/2)_\mathrm{u}$ state will eventually relax to the electronic ground state of the Kr_2^+ ion and this relaxation, if combined with a quite efficient transition form $\mathrm{II}(1/2)_\mathrm{g}$ to $\mathrm{II}(1/2)_\mathrm{u}$, may thus lead to an observable depletion of the group II states in experimental Kr_2^+ populations. We will return to this interesting point once more in the following subsection.

B. Model evolutions of electronic excitations in Kr_2^+

To analyze the processes leading to the relaxation of initial electronic excitations in the Kr_2^+ ion in a more illustrative way, we present, in this subsection, a series of model time evolutions of occupations of electronic states in Kr_2^+ starting from specific electronic states. The evolutions have been calculated using rate constants obtained for $T = 300\,\mathrm{K}$ and for the carrier gas density corresponding to $P = 760\,\mathrm{Torr}$. The methodology described in Subsec. II C has been used with both spontaneous radiative and collision-induced processes considered, though the former, as discussed above, contribute only marginally.

The results of performed calculations are summarized in Figs. 4–6 in which three representative values of the reduced electric field are considered, a low one ($E/N = 5\,\mathrm{Td}$) representing the $E/N \to 0$ (thermal) limit and other two ($E/N = 300\,\mathrm{Td}$ $E/N = 1000\,\mathrm{Td}$) representing stronger electric fields (higher collision energies) where dimer ion disappearance processes become gradually important.

1. Weak-field region

Selected Kr_2^+ electronic relaxation evolutions predicted for $E/N = 5\,\mathrm{Td}$ are depicted in Fig. 4. As expected from the observations discussed in the preceding subsection, already a first glance at the recorded time profiles reveals quite distinct features seen for processes started from group I electronic states and those started from group II states.

For the ground state, $\mathrm{I}(1/2)_\mathrm{u}$, no visible evolution has been recorded on the time scale considered. Since the transitions to higher electronic states are completely negligible and the same holds for the ion disappearance rate, the initially populated ground state does not change along the whole recorded evolution and also no visible decrease of the dimer abundance is seen.

For the other group I states, a different picture is seen since a) the electronically excited dimer ions may disappear (dissociate) much easily than the ground state due to a considerably reduced binding energy and b) downward collision-induced electronic transitions are quite efficient even in the $E/N \to 0$ limit (see Fig. 3). A common feature observed for all the initial electronic excitations belonging to group I is that the Kr_2^+ ion always relaxes, quite fast ($t \leq 10^{-3}\,\mu$s), to the electronic ground state (with intermediate, lower lying electronic states always involved).

The evolutions recorded for group II states are mainly governed by the dimer ion disappearance which leads to a quite considerable decrease of the dimer abundance. However, the conversion of the initial electronic excitation to the electronic ground state is also observed in survived dimers, either directly if the evolution starts from the $\mathrm{II}(1/2)_\mathrm{u}$ state, or indirectly through the $\mathrm{II}(1/2)_\mathrm{u}$ states if the evolution starts from the $\mathrm{II}(1/2)_\mathrm{g}$ state. Noteworthy, intermediate group I states are skipped (their normalized abundances are well below 10^{-4}). The non-zero value of the rate constant of the $\mathrm{II}(1/2)_\mathrm{u} \to \mathrm{I}(1/2)_\mathrm{u}$ transition is clearly responsible for the observed group II to group I conversion and, thus, the break of the quasiadiabaticity of the underlying processes. Since, on the other hand, the value of this rate constant is much smaller than the value of the rate constant of the $\mathrm{II}(1/2)_\mathrm{g} \to \mathrm{II}(1/2)_\mathrm{u}$ transition, the evolution still remains quasiadiabatic at short time-scales (up to about $t \approx 10^{-3}\,\mu$s) and the quasiadiabaticity is thus violated only at times about an order of magnitudes longer ($t \geq 10^{-2}\,\mu$s).

2. Strong-field region

In the case of a strong external electric field, a somewhat different picture is seen (see Figs. 5 and 6), mainly because the efficiency of the collision-induced dimer ion disappearance becomes, even for the most bound $\mathrm{I}(1/2)_\mathrm{u}$ and $\mathrm{I}(3/2)_\mathrm{g}$ states, gradually enhanced.

While, for the initial electronic excitations belonging to group I, their subsequent relaxation roughly follows the patterns observed at weak electric fields, two major differences are observed. Firstly, the role of intermediate, lower-lying states is gradually reduced as E/N increases, and, secondly, the dimer ion disappearance is efficient enough to completely sweep out the initial population of dimers within a fairly short time. As a consequence, it seems that, in stronger electric fields, two main processes compete when group I electronic exci-

tations are relaxed: a) a direct (and fast) conversion of the initial electronic excited state to the electronic ground state and a subsequent (somewhat slower) decay of the ground-state dimer, and b) a direct decay of the excited dimer. The latter mechanism seems to be the more efficient, the higher is the initial excitation.

The situation further simplifies if the initial electronic excitation concerns the group II states. In this case, the role of intermediate electronic states is heavily suppressed and the dimer ion disappearance completely dominates. Noteworthy, however, the traces of the Kr_2^+ ions that survive up to long times almost exclusively populate the electronic ground state.

3. Relevance of Kr_2^+ *excited electronic states*

To estimate the effect of particular electronic excitations of Kr_2^+ on the transport and other macroscopic properties of the dimer ions in krypton gas, we have estimated the number of collisions the dimer ions undergo with krypton atoms before they change their electronic state and/or disappear (dissociate). In general, one may suppose that the effect will be the more pronounced, the larger is the number of such collisions.

In weak electric fields, all the initial electronic excitations are eventually converted in the Kr_2^+ ion to the electronic ground state, $I(1/2)_u$, unless the ion disappears (dissociates). However, while a typical relaxation time is below $t \approx 10^{-3}\,\mu$s for the initial Kr_2^+ electronic excitations belonging to group I, it increases considerably if group II excitations are involved (up to $t \approx 10^{-2} - 10^{-1}\,\mu$s). It means that group II excitations may survive quite long in Kr_2^+ ions for the excited ions to undergo a significant number of collisions with carrier gas atoms and to contribute to observed macroscopic features (e.g., transport properties) of experimental Kr_2^+ populations.

More specifically, the total mean collision frequency of Kr_2^+/Kr collisions is estimated, at ambient conditions and for $E/N = 5\,$Td, to about $\nu_{\mathrm{coll}} \approx 10^5\,\mu\mathrm{s}^{-1}$. Then, a Kr_2^+ ion initially excited to the $II(1/2)_u$ state, which is expected to survive for $t \approx 10^{-2} - 10^{-1}\,\mu$s, should undergo about $10^3 - 10^4$ collisions with neighboring Kr atoms. A dimer ion created in the $II(1/2)_g$ state, on the other hand, is expected to undergo much less Kr_2^+/Kr collisions (dozens, a comparable number one gets for the group I electronic excitations) since its life time is much shorter (about $t \approx 10^{-4} - 10^{-3}\,\mu$s). However, a non-negligible amount

of Kr_2^+ ions occupying the $II(1/2)_u$ state results from ions initially excited to the $II(1/2)_g$ state and these $II(1/2)_u$ ions participate, afterwards, in thousands of collisions before they dissociate and/or relax to the electronic ground state. As a consequence, ion dimers electronically excited to the group II states, the $II(1/2)_u$ state in particular, are expected to play a role in weak electric fields and should be considered in the analysis and interpretation of experimental data.

In the strong field region, a very fast depletion of the initial population of Kr_2^+ is observed for both the electronic ground-state dimer as well as initially electronically excited dimers, typical disappearance times being about $t \approx 10^{-3}\,\mu$s for the ground state and $t \approx 10^{-4}\,\mu$s for excited states. As a consequence, molecular Kr_2^+ ions are expected to play only a limited role in cold krypton plasmas if strong electric fields are applied. However, since, e.g., for $E/N = 1000\,$Td, the total mean collision frequency is estimated to $\nu_{\rm coll} \approx 10^6\,\mu{\rm s}^{-1}$, the decaying dimer ions may still undergo about several dozens (electronically excited) to several hundreds (ground-state dimer ions) of collisions before they disappear. Since the life time of the ions in their electronic ground state is estimated to be only about an order of magnitude longer than those obtained for electronically excited ions, some effect of the latter cannot be excluded, but will probably not be much important. Naturally, the recombination processes of Eqs. (1) and (2) may influence the final picture. However, in the strong field region, they are expected to be much less important than in weak electric fields and, consequently, only a slight effect is presumed from them. Unfortunately, no data are presently available on the recombination rates to make any quantitative assessment.

IV. SUMMARY AND CONCLUSIONS

Outputs of preceding dynamical calculations on Kr_2^+/Kr collisions occurring in cold krypton plasma [19, 20] have been re-analyzed to get effective cross-sections and rate constants of collision-induced inter-state transitions in Kr_2^+ ions. In addition, rate constants of inter-state transitions resulting from spontaneous radiative processes occurring in electronically excited Kr_2^+ ions have also been calculated using a semiclassical approach based on the classical treatment of nuclei and a full quantum description of electrons. All the relevant low-lying electronic states of the Kr_2^+ ion have been taken into account, namely the $I(1/2)_u$ ground state, excited states asymptotically correlating to the fine-structure ground state ($^2P_{3/2}$) of

the atomic ion, $I(3/2)_g$, $I(3/2)_u$ and $I(1/2)_g$ (group I states), and excited states asymptotically correlating to the Kr^+ fine-structure excited state ($^2P_{1/2}$), $II(1/2)_u$ and $II(1/2)_g$ (group II states). For simplicity and practicability of presented calculations, only rotationally-vibrationally ground states of the Kr_2^+ ion have been considered on respective potential energy curves.

The calculated rate constants have subsequently been used in kinetic modelings of electronic relaxation processes in Kr_2^+ ions, initially prepared in a specific electronic state, and their decay. All the modelings have been performed at ambient conditions ($T = 300\,\mathrm{K}$ and $P = 760\,\mathrm{Torr}$) and two representative external electric fields, $E/N = 5\,\mathrm{Td}$ representing the weak-field (thermal) limit and $E/N = 1000\,\mathrm{Td}$ representing the strong-field (high collision energy) limit. It is noteworthy that the radiative processes are much less efficient under these conditions than the non-radiative, collision-induced ones and that a considerable dilution of the carrier gas (by 2 to 6 orders of magnitude, in dependence on the particular transition) would be required to make the radiative processes competitive.

For the weak-field region, it has been found that all the possible initial Kr_2^+ electronic excitations eventually relax to the dimer electronic ground state. This relaxation is faster for group I excitations ($t \approx 10^{-3}\,\mu\mathrm{s}$) than for group II excitations ($t \approx 10^{-2} - 10^{-1}\,\mu\mathrm{s}$). In particular for the group II excitations, the electronic relaxation seems to be slow enough so that the excited dimer ions may influence macroscopic properties of cold krypton plasmas recorded in weak electric fields. It should be also noted, however, that the dimer disappearance (dissociation) becomes increasingly important as the electronic excitation increases. For example, for the group II excitations, the dimer ions that survive up to $t = 1\,\mu\mathrm{s}$ represent only 20 % of their initial population for the $II(1/2)_u$ initial state or even only 5 % for the $II(1/2)_g$ initial excitation. Interestingly, the electronic relaxation starting in group II skips group I intermediate states and is relaxed to the dimer ground state either via a direct, $II(1/2)_u \rightarrow I(1/2)_u$ transition for the $II(1/2)_u$ initial excitation or via a bit more involved pathway, $II(1/2)_g \rightarrow II(1/2)_u \rightarrow I(1/2)_u$, if the relaxation starts from $II(1/2)_g$.

In the strong-field region, the processes governing the evolution of electronically excited Kr_2^+ are completely dominated by a quite fast decay of the dimers. While the decay of electronically ground-state dimer ions is somewhat slower ($t \approx 10^{-3}\,\mu\mathrm{s}$) than the dissociation of electronically excited ions ($t \approx 10^{-4}\,\mu\mathrm{s}$), the life times of excited states are almost independent on the particular Kr_2^+ electronic excitation. Like in weak fields, the dimer decay

processes include, to some small extent, intermediate electronic states if started from a group I excited state. The group II excitations lead, on the other hand, to a direct dissociation and no intermediate states are observed at a non-negligible abundance.

Preliminary calculations (not reported in this work) seem to indicate that the efficiency of inter-group transitions is considerably reduced if the dimer ion is rotationally-vibrationally excited and, thus, the rotational-vibrational excitations of the dimer will highly probably enhance the role the electronically excited dimers play in cold krypton plasmas. However, a more extensive calculations heavily exceeding the scope of the present work would be needed to provide a reliable assessment of the effect the Kr_2^+ rotational-vibrational excitations have on experimental data.

Last but not least, since processes leading to the formation of krypton dimer ions (e.g., ternary recombination collisions) have not been taken into account in the present work, a complete description of the formation and quenching of electronic excitations in the Kr_2^+ ion in cold krypton plasmas has still not been achieved. Among others, it means that the present data do not allow, by themselves, to estimate the abundances of Kr_2^+ electronic states in cold krypton plasmas and are, thus, not sufficient to resolve the question about the role of electronically excited dimer ions in these plasmas as raised in a preceding publication [20]. Presently, additional calculations focused on the formation of the Kr_2^+ ions are being prepared in our group. Beyond that, however, the present work on the rate constants of processes involving different Kr_2^+ electronic states can be directly used in, for instance, the electrodynamics modeling of low temperature plasma jets in krypton gas where the plasma active species are governed by the directed streamer development having both a low field region (a few Td) in the streamer channel and a strong field region (a few hundreds of Td) in the streamer head. For this, the rate constants governing the krypton dimer ion populations have been provided and analyzed for both weak-field and strong-field conditions.

Acknowledgments

René Kalus and Cyril Van de Steen express their thanks to the Ministry of Education, Youth and Sports of the Czech Republic for the financial support from the *National Programme of Sustainability* (NPS II) project (grant no. LQ1602) and the *Large Infrastructures for Research, Experimental Development and Innovations* project (grant

no. LM2015070), as well as to VSB-TUO (grant no. SP2018/178). Traveling support from the Barrande programme of French-Czech collaboration (grants no. 40688TH and 8J18FR031) is also warmly acknowledged. The calculations have been performed using the resources of the IT4Innovations National Supercomputing Center of the Czech Republic (grant no. OPEN-13-2) and multiprocessing work stations of the parallel computational center of Toulouse.

[1] M. Laroussi, IEEE Trans. Plasma Sci. **37**, 714 (2009).

[2] M. Yousfi, N. Merbahi, A. Pathak, and O. Eichwald, Fund. Clin. Pharm. **28**, 123 (2014).

[3] H. Tanaka, K. Ishikawa, M. Mizuno, S. Toyokuni, M. Kajiyama, F. K. and. H.-R. Metelmann, and M. Hori, Rev. Mod. Plasma Phys. **3**, 1 (2017).

[4] A. I. Bugrova, A. M. Bishaev, A. V. Desyatskov, M. V. Kozintseva, A. S. Lipatov, and M. Dudeck, Int. J. of Aero. Eng. **2013**, ID 686132 (2013).

[5] S. Mazouffre, Plasma Sources Sci. Technol. **25**, 033002 (2016).

[6] H. Helm and M. T. Elford, J. Phys. B **11**, 3939 (1978).

[7] H. Helm, Phys. Rev. A **14**, 680 (1976).

[8] C. Praxmarer, A. Hansel, A. Jordan, H. Kraus, and W. Lindinger, Int. J. Mass Spec. Ion. Proc. **129**, 121 (1993).

[9] T.-K. Ha, P. Rupper, A. Wuest, and F. Merkt, Mol. Phys. **101**, 827 (2003).

[10] R. Kalus, I. Paidarová, D. Hrivňák, P. Paška, and F. X. Gadéa, J. Chem. Phys **294**, 141 (2003).

[11] A. K. Dham, A. R. Allnatt, W. J. Meath, and R. A. Aziz, Mol. Phys. **67**, 1291 (1989).

[12] R. Kalus, Collect. Czech. Chem. Commun. **65**, 141 (2000).

[13] H. Helm, J. Phys. B **9**, 2931 (1976).

[14] M. Tomza, K. Jachymski, R. Gerritsma, A. Negretti, T. Calarco, Z. Idziaszek, and P. S. Julienne, Rev. Mod. Phys **91**, 035001 (2019).

[15] A. D. Dörfler, P. Eberle, D. Koner, M. Tomza, M. Meuwly, and S. Willitsch, Rev. Mod. Phys (2019), 1906.12285.

[16] L. Ratschbacher, C. Zipkes, C. Sias, and M. Köhl, Nature Phys **8**, 649 (2012).

[17] J. Joger, H. Fürst, N. Ewald, T. Feldker, M. Tomza, and R. Gerritsma, Phys. Rev. A **96**,

030703 (2017).

[18] R. Saito, S. Haze, M. Sasakawa, R. Nakai, M. Raoult, H. D. Silva, O. Dulieu, and T. Mukaiyama, Phys. Rev. A **95**, 032709 (2017).

[19] C. Van de Steen, M. Benhenni, R. Kalus, R. Ćosić, S. Illésová, F. X. Gadéa, and M. Yousfi, Plasma Sources Sci. Technol. **28**, 035007 (2019).

[20] C. Van de Steen, M. Benhenni, R. Kalus, R. Ćosić, F. X. Gadéa, and M. Yousfi, Plasma Sources Sci. Technol. (2019), https://doi.org/10.1088/1361-6595/ab3a17.

[21] I. Janeček, M. Stachoň, F. X. Gadéa, and R. Kalus, Phys. Chem. Chem. Phys. **19**, 25423 (2017).

[22] As discussed elsewhere [21], radiative processes do not play an important role during the collision compared to non-radiative processes and are thus neglected here. Moreover, since under ambient conditions the time during which the dimer ion undergoes collisions is much shorter than the time it spends as a free molecule, the effect of radiative processes taking place during the collisions may, in addition, be also considered negligible with respect to the free-flight phase. The probability of free-flight non-radiative transitions in the Kr_2^+ ion is, on the other hand, zero if the spin-orbit coupling is neglected and is almost zero if the spin-orbit coupling is included via the atoms-in-molecules scheme (as done in the present work). As a consequence, the non-radiative free-flight transitions in the Kr_2^+ ion are neither considered in the present work.

[23] Mostly, the dimer disappearance means that the collisionally excited dimer disscociates, $Kr_2^+ + Kr \rightarrow Kr^+ + 2Kr$. However, as discussed in detail in Ref. [20], the dimer-to-monomer charge transfer, $Kr_2^+ + Kr \rightarrow Kr^+ + Kr_2$, leading to the same ionic fragment as the dimer dissociation, may also play a role if specific electronic states of the dimer ion are populated prior to collision. the dimer disappearance channel is thus introduced to represent both reaction mechanisms leading to the monomer ion product without explicitly discriminating between them.

[24] In this work, we use the following numerical labels to specify the electronic state of the ionic dimer: $\alpha = 1$ for $I(1/2)_u$, $\alpha = 2$ for $I(3/2)_g$, $\alpha = 3$ for $I(3/2)_u$, $\alpha = 4$ for $I(1/2)_g$, $\alpha = 5$ for $II(1/2)_u$, and $\alpha = 6$ for $II(1/2)_g$.

[25] In general (see, e.g., Ref. 19), distances in the dimer are sampled from (squares of) nuclear wave functions obtained for a given rotational-vibrational state (ground state in this work) by numerically solving two-particle Schrödinger equation for the two krypton nuclei. Afterwards,

nuclear velocities are added in the perpendicular direction to the dimer bond axis to get required rotational angular momentum (does not apply in this work) and along the bond axis to get the required rotational-vibrational energy (zero-point vibration energy in this work).

[26] M. Yousfi, A. Hennad, and O. Eichwald, J. of Appl. Phys. **84**, 107 (1998).

[27] In weakly ionized gas, the ionization degree of about 10^{-6} to 10^{-5} is presumed. It is thus clear that the concentration of electrons is necessarily much lower (by 5 to 6 orders of magnitude) than the concentration of the background gas. Despite the fact that the electron-dimer dissociative recombination has much higher frequency than the dimer-atom collisions (by 1 to 3 order of magnitudes), the effect of dimer collisions with background gas atoms completely prevails over collisions with free electrons.

[28] E. Fermi, *Nuclear Physics* (The University of Chicago Press, Chicago, 1950).

[29] All the (binary) collision-induced processes are considered, in this work, as first-order ones since the particle density of the carrier gas, n_{g}, enters the kinetic equations as a (presumably constant) parameter. Since related rate constants are multiplied by this constant carrier-gas density in Eqs. (14), they are presented in this multiplied form throughout this paper. The radiative rate constants, on the other hand, enter Eqs. (14) as they are and will thus be presented in the same way (i.e., not multiplied by n_{g}).

[30] Below in the kinetic modeling part of this section (Subsec. III B), the radiative processes have always been considered. However, no visible changes in calculated time evolutions have been observed after the radiative rate constants were set to zero.

Figures and Tables

TABLE I: Rate constants (k) and half-times ($\tau = \ln 2/k$) of radiative transitions in the rotationally-vibrationally ground-state Kr_2^+ ion, $[j = 0, v = 0]$, as given by Eqs. (10)–(12).

transition	k [μs^{-1}]	τ [μs]
$II(1/2)_g \rightarrow II(1/2)_u$	0.0009	790
$II(1/2)_g \rightarrow I(1/2)_u$	0.0949	7.3
$I(3/2)_u \rightarrow I(3/2)_g$	0.0050	138
$I(1/2)_g \rightarrow I(1/2)_u$	0.0006	1137
$II(1/2)_u \rightarrow I(1/2)_g$	0.4347	1.6

FIG. 1: Potential energy curves of the lowest-lying electronic states of the Kr_2^+ ion (taken and adapted from Ref. [20]).

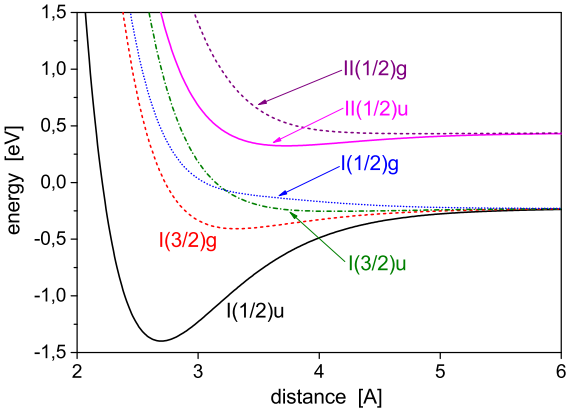


FIG. 2: Normalized rate constants of collision-induced dimer ion disappearance, $n_g k_\alpha^{(4)}$, calculated for rotationally-vibrationally ground-state Kr_2^+ dimers, $[j = 0, v = 0]$, in respective electronic states (group I – open symbols, group II – full symbols) and at room temperature ($T = 300\,\mathrm{K}$). Note that the rate constants are multiplied (see Subsec. II C) by the carrier-gas particle density corresponding to the atmospheric pressure ($P = 760\,\mathrm{Torr}$) and room temperature. For comparison, rate constants of spontaneous radiative dissociation of the Kr_2^+ ion (not multiplied by the gas density) are also provided as horizontal lines framed with respective symbols.

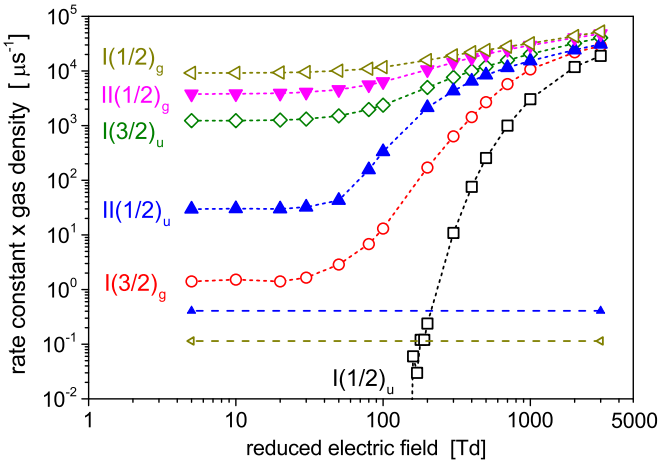


FIG. 3: Normalized rate constants of collision-induced inter-state transitions, $n_g k^{(3)}_{\alpha\beta}$, calculated for rotationally-vibrationally ground-state Kr_2^+ dimers, $[j = 0, v = 0]$, initially created in electronic states indicated in respective panels and for room temperature ($T = 300\,\mathrm{K}$). Like in Fig. 2, the rate constants are multiplied by the carrier-gas particle density set to the value corresponding to $P = 760\,\mathrm{Torr}$ and room temperature. Rate constants of inter-state transitions due to spontaneous radiative processes in Kr_2^+ (not multiplied by the gas density) are also provided as dashed horizontal lines framed with respective symbols. If a particular curve is missing in any panel, the corresponding rate constant is equal to zero for all the values of the reduced electric field considered.

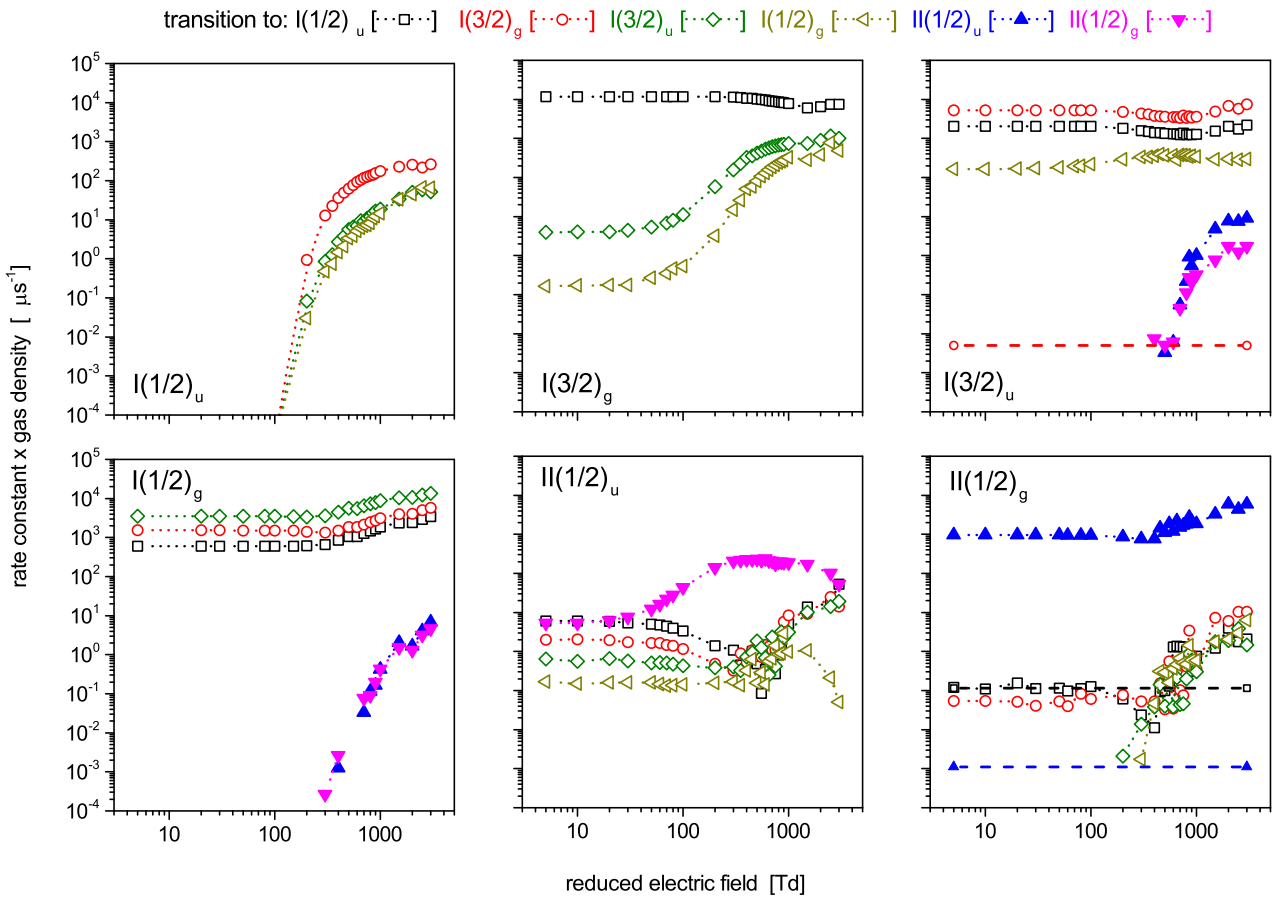


FIG. 4: Time evolutions of normalized abundances of Kr_2^+ electronic states [$n_\alpha(t)/n_0$, where n_0 is the total Kr_2^+ density at $t = 0$] in populations of ionic dimers initially populating a particular electronic state (indicated on the right of each panel) as calculated for $E/N = 5\,\mathrm{Td}$. Note that the processes leading to the creation of the Kr_2^+ dimer [Eqs. (1) and (2)] are not considered in this figure. For this reason, time evolutions of $n(t)/n_0$ [$n(t) = \sum_\alpha n_\alpha(t)$] are also shown (thick gray lines) to visualize the progress of the dimer ion disappearance. Note also that the rotational-vibrational ground state is assumed to be unchanged in Kr_2^+ for all the considered times.

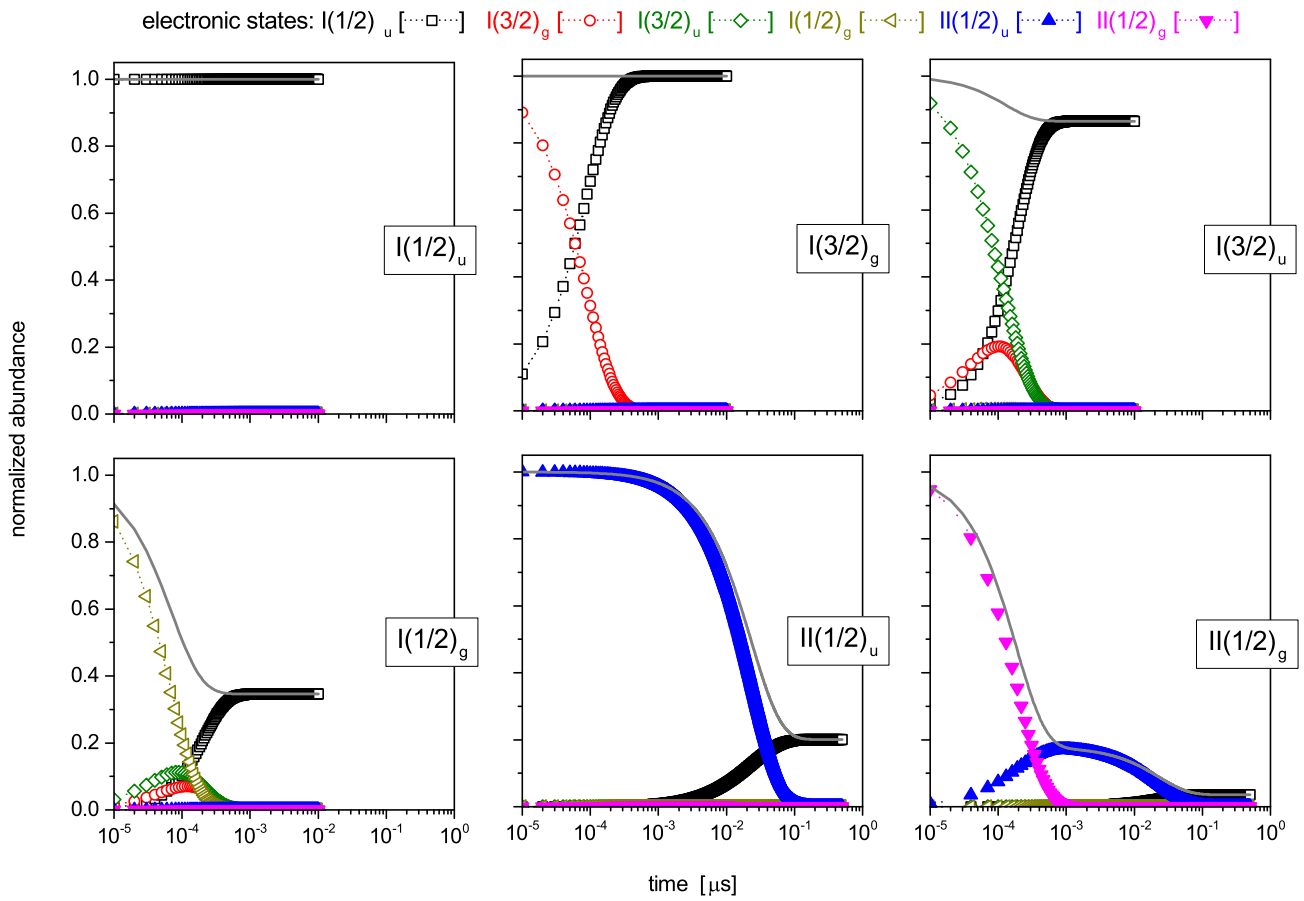


FIG. 5: The same as in Fig. 4, but calculated for $E/N = 300\,\mathrm{Td}$.

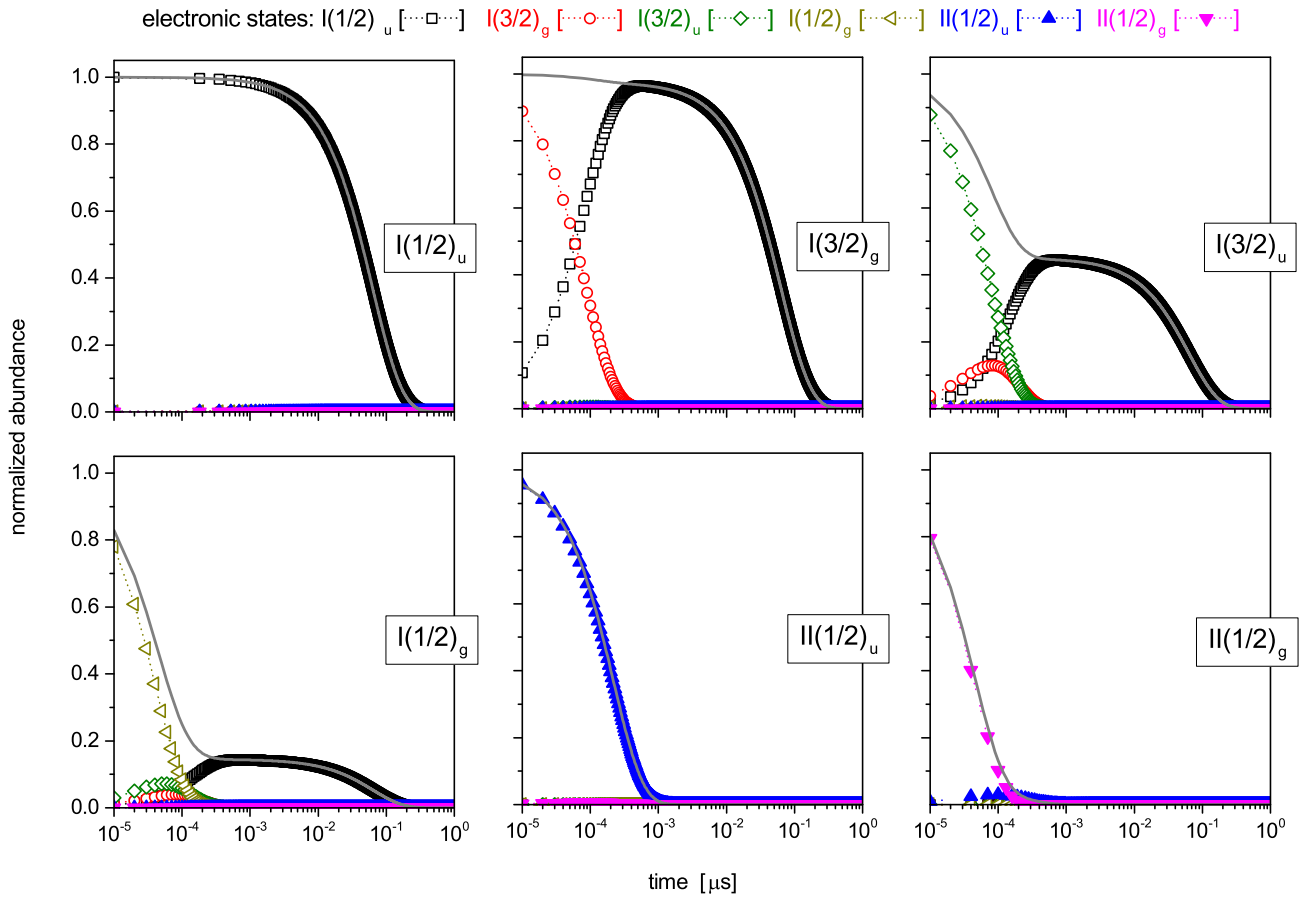
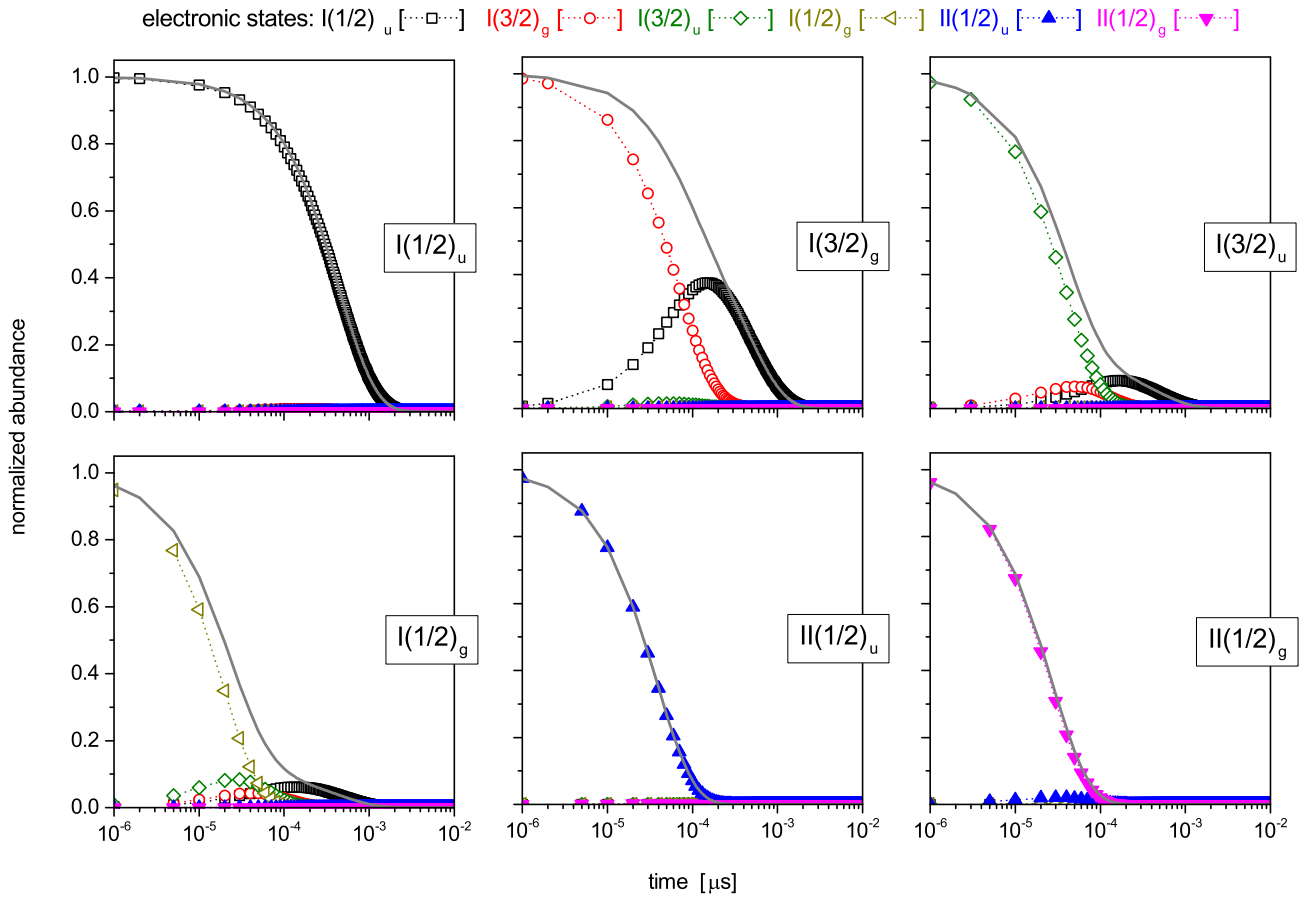


FIG. 6: The same as in Fig. 4, but calculated for $E/N = 1000\,\mathrm{Td}$. **(Note that a different time scale is used in this figure.)**



APS/123-QED

Relaxation of electronic excitations in Kr_2^+ ions in cold krypton plasma.

Cyril Van de Steen,[1,2,*] Malika Benhenni,[2,†] René Kalus,[1,‡]
Rajko Ćosić,[1,3] Florent Xavier Gadéa,[4] and Mohammed Yousfi[2]

[1]*IT4Innovations, VSB - Technical University of Ostrava, 17. listopadu 2172/15, 708 00 Ostrava-Poruba, Czech Republic.*

[2]*Laboratoire Plasma et Conversion d'Energie, LAPLACE & UMR5213 du CNRS, Université de Toulouse III Paul Sabatier, 118 route de Narbonne, 31062 Toulouse Cedex, France.*

[3]*Department of Applied Mathematics, Faculty of Electrical Engineering and Computer Science, VSB - Technical University of Ostrava, 17. listopadu 2172/15, 708 00 Ostrava-Poruba, Czech Republic.*

[4]*Laboratoire de Chimie et de Physique Quantiques, IRSAMC & UMR5626 du CNRS, Université de Toulouse III Paul Sabatier, 31062 Toulouse Cedex 09, France.*

(Dated: November 20, 2019)

Abstract

Reaction rate constants have been calculated for electronic transitions in Kr_2^+ ions and for their decay as induced by collisions with krypton atoms and/or spontaneous radiation processes. The rate constants have then been used in a series of modelings of electronic relaxation in the ions in cold krypton plasmas with the main focus on relaxation times and final states. It has been shown that the collision-induced (non-radiative) relaxation is much faster than the radiative one and completely dominates with typical relaxation times ranging between nanoseconds and microseconds. The relaxation always ends up in the Kr_2^+ electronic ground state, high electronic excitations survive for longer times than lower excitations due to spin-orbit coupling effects.

PACS numbers: 52.20.-j 52.20.Hv 34.50.-s

*Electronic address: cyril.vds@gmail.com

[†]Electronic address: malika.benhenni@laplace.univ-tlse.fr
[‡]Electronic address: rene.kalus@vsb.cz

I. INTRODUCTION

Cold rare-gas plasmas have recently received a considerable attention raised by a promising potential in various applications. Among others, biomedicine [1–3] and spacecraft propulsion [4, 5] may serve as the most pronounced examples. In complement to the experimental research, numerical modeling plays an important role in plasma physics, mainly because they are able to provide a deep insight into phenomena and processes not usually accessible by experiments. It is particularly important for rare-gas plasmas since various aspects of their physics are to be deeply understood in order to control and tailor their properties important for their efficient applications. For example, the formation of active species (radicals, excited species, charged particles etc.) and the basic data on their reactivity and transport are of particular importance in fluid dynamics modelings of cold rare-gas plasmas and tailoring their characteristics.

Ions of various kinds have a major effect on the magnitude of the space charge electric field and, in turn, are determinant or even decisive for the formation and the densities of many other active species in cold plasmas. In rare-gas plasmas, in particular, atomic ions would primarily be expected to be by far the most abundant ones and, thus, to play the most important role in influencing plasmas properties. However, it was shown a long time ago [6–8] that molecular ions of small sizes, namely, dimers and trimers, also play a significant role, which is a clear consequence of their rather strong binding. Specifically, the krypton dimer ion, Kr_2^+, may serve as a good example with its binding being of almost chemical strength ($D_0 \approx 1.15\,\mathrm{eV}$) [9, 10]. This stands in a clear contrast to the neutral krypton dimer, Kr_2, the binding energy of which is too small ($D_0 \approx 0.016\,\mathrm{eV}$ [11]) for the Kr_2 molecule to survive, at ambient conditions, at a non-negligible amount [12].

The krypton dimer ion cannot thus arise from a direct ionization of its neutral precursor and alternative mechanisms were also proposed [6]: a) the *three-body recombination*,

$$\mathrm{Rg}^+ + \mathrm{Rg} + \mathrm{Rg} \rightarrow \mathrm{Rg}_2^+ + \mathrm{Rg} \tag{1}$$

and b) the *associative ionization* (the asterisk on the left-hand-side denotes electronic excitation),

$$\mathrm{Rg}^* + \mathrm{Rg} \rightarrow \mathrm{Rg}_2^+ + \mathrm{e}^-, \tag{2}$$

the latter being also called the *Hornbeck-Molnar process*. Since electronically excited

monomers participate on the reactant side not only in the reaction given by Eq. (2), but also in the three-body recombination process [13], electronically excited products (dimer ions) are highly probably to be produced and the initial electronic excitation is only afterwards relaxed. However, the processes of such relaxation cannot be easily monitored experimentally and theoretical modeling is thus strongly needed. **The relaxation of electronic excitations in atomic and molecular ions colliding with atoms has also been studied elsewhere [14–18], however the context of cold atoms physics is quite different from the cold plasma one, and mainly charge transfer processes were investigated in these works.**

In two preceding papers [19, 20] we have investigated transport properties of the krypton dimer ion in the electronic ground state [19] and low-lying excited states [20]. Since the results we obtained are compatible for both ground-state and excited-state dimers with available experimental data [6], both types of the Kr_2^+ dimer may be present in experimental populations. However, the experimental data do not allow to make an (at least rough) quantitative estimate of how various electronic excitations are populated in Kr_2^+ under typical experimental conditions.

The abundances of particular electronic states are basically influenced by two factors: a) the way how the Kr_2^+ ions are formed and b) how the nascent population of electronic excitations is afterward relaxed. In the present work, we focus on the latter issue and provide an introductory study of processes responsible for the relaxation of the nascent electronic excitation in krypton dimer ions. It is noteworthy that both spontaneous radiative transitions as well as non-radiative, collision-induced processes may in principle play a role and are, thus, considered.

The results reported in the present paper are mostly based on our preceding dynamical calculations on the Kr_2^+/Kr collisions [19, 20], the outputs of which have been analyzed in a more detailed way here, however, which has enabled detection of particular electronic states on the output. This has allowed to assess all the parameters governing the relaxation of the initial electronic excitation in the Kr_2^+ ion, namely, effective collision cross-sections of state-to-state transitions and related rate constants. The calculated rate constants have then been used, together with rate constants of radiative transitions calculated here using a semiclassical approach (see Sec. II B 2) and rate constants of collision-induced dimer ion disappearance reported in preceding studies [19, 20], in kinetic modelings of electronic

relaxation in Kr_2^+.

It should be noted that the considered reaction rate constants may in general depend on the initial rotational-vibrational excitation of the ionic dimer. Therefore, they have to be properly averaged over the rotational-vibrational states following, e.g., thermal distributions. However, such a full calculation considering both the (six) electronic states and (dozens of) rotational-vibrational states of the ionic dimer is clearly beyond the scope of the present work. For simplicity and to avoid calculations of impracticable extent, only the rotational-vibrational ground state, $[j = 0, v = 0]$, has been considered for each Kr_2^+ electronic state. Despite this, we believe that the results obtained may still provide qualitatively sound, or even semi-quantitative estimates of the efficiency of the electronic relaxation in Kr_2^+ and the relevance of particular electronic states in Kr_2^+ populations in cold krypton plasmas.

The present paper is organized as follows. First, methodological approaches and computations are reviewed in Sec. II. Specifically, processes considered in the present model of the electronic relaxation in Kr_2^+ are summarized in Subsec. II A, the methods of the calculation of needed rate constants are discussed in Subsec. II B, and, finally, kinetic equations governing the electronic relaxation in Kr_2^+ are introduced and methods for their solution are described in Subsec. II C. Then, main results are presented and discussed in Sec. III, with calculated rate constants summarized in Subsec. III A and typical relaxation evolutions of selected nascent populations of electronic excitations in Kr_2^+ discussed in Subsec. III B. Finally, conclusive remarks and outlooks are provided in Sec. IV.

II. METHODS AND COMPUTATIONS

A. Processes

The following low-lying electronic states of the Kr_2^+ ion and transitions among them have been considered, the $\mathbf{I(1/2)_u}$ ground state, excited states asymptotically correlating to the fine-structure ground state ($^2P_{3/2}$) of the atomic ion, $\mathbf{I(3/2)_g}$, $\mathbf{I(3/2)_u}$ and $\mathbf{I(1/2)_g}$ (group I states), and excited states asymptotically correlating to the Kr^+ fine-structure excited state ($^2P_{1/2}$), $\mathbf{II(1/2)_u}$ and $\mathbf{II(1/2)_g}$ (group II states). A graphical summary of them is provided in Fig. 1.

Two kinds of transition processes are considered in the present work, (non-radiative)

collision-induced transitions and *spontaneous radiative transitions* in free ionic dimers. **As discussed elsewhere [21], radiative processes do not play an important role during the collision compared to non-radiative processes and are thus neglected here [22]. Since, in addition, the probability of non-radiative transitions is very small in free Kr_2^+ ions (exactly zero if the spin-orbit coupling is neglected), the non-radiative free-flight transitions are neither considered here.**

Both collision-induced processes and spontaneous radiative processes may result either in an electronic transition in the dimer ion or in the dimer ion disappearance, the latter mainly due to dimer dissociation [23] **and, consequently, the following processes have to be considered** (small Greek letters represent particular electronic states of the dimer [24]):

collision-induced inter-state transition (cIST),

$$\mathrm{Kr}_2^+(\alpha) + \mathrm{Kr} \rightarrow \mathrm{Kr}_2^+(\beta) + \mathrm{Kr}, \tag{3}$$

collision-induced dimer ion disappearance (cDID),

$$\mathrm{Kr}_2^+(\alpha) + \mathrm{Kr} \rightarrow \mathrm{Kr}^+ + 2\mathrm{Kr}/\mathrm{Kr}_2, \tag{4}$$

radiative inter-state transition (rIST),

$$\mathrm{Kr}_2^+(\alpha) \rightarrow \mathrm{Kr}_2^+(\beta) + h\nu, \tag{5}$$

and *radiative dimer dissociation* (rDD)

$$\mathrm{Kr}_2^+(\alpha) \rightarrow \mathrm{Kr}^+ + \mathrm{Kr} + h\nu. \tag{6}$$

Note that the two latter processes are used to discriminate between radiative transitions resulting to a stabilized dimer on the output, Eq. (5), and transitions from a bound rotational-vibrational state to a continuum state leading to dimer dissociation, Eq. (6).

All the processes given by Eqs. (3)–(6) are considered in the present work with related rate constants denoted as $k_{\alpha\beta}^{(3)}$, $k_{\alpha}^{(4)}$, $k_{\alpha\beta}^{(5)}$, and $k_{\alpha}^{(6)}$, respectively, where the upper index indicates the number of the equation describing each particular process.

B. Reaction rate constants

1. *Rate constants of collision-induced processes*

The present calculations related to the collision-induced processes, Eqs. (3) and (4), heavily rely on the data reported in the preceding studies on the Kr_2^+/Kr collisions [19, 20]. To summarize, let us recall that, in those studies, we calculated bunches of Kr_2^+/Kr (quasiclassical) collision trajectories for the dimer ion being, prior to a collision, either in its electronic ground state [$I(1/2)_u$] or in one of the five lowest excited states [$I(3/2)_g$, $I(3/2)_u$, $I(1/2)_g$, $II(1/2)_u$, and $II(1/2)_g$]. For each electronic state, a broad range of (center-of-mass) collision energies was considered (between $E_{coll} = 0.01\,eV$ and $E_{coll} = 100\,eV$), and, for each collision energy, a sufficiently large number of impact-parameter values were included and sampled between $b = 0$ and $b = b_{max}$ ($b_{max} = 10{-}30\,Å$, depending on the electronic state and collision energy) with a step of $\Delta b = 0.1\,Å$. Altogether 528 trajectories were integrated numerically for each value of the impact-parameter. They started from a sample of Kr_2^+/Kr initial conditions imitating experimental conditions and covering various (isotropic) orientations of the dimer ion in space and various phases of its rotational-vibrational motion [25]. **Note also that the forces due to the external electric field are completely negligible compared to inter-atomic interactions and, consequently, the external electric field has not been considered in trajectory calculations.**

Totally, 50,000 to 150,000 trajectories were evaluated for each collision energy and electronic state, and subsequently were used to evaluate effective cross-sections of particular collision channels. Following the conclusions of an immediately preceding study [20], electronic potentials of Ref. 9 (referred therein as model B) have been used in calculations on the Kr_2^+ ion starting from the electronic ground state and the potentials of Ref. 10 (model A) have been employed for electronically excited dimers.

The rate constants of cDID processes, Eq. (4), were calculated in the two preceding studies [19, 20] and are used here without any additional modification.

Alike, most of the data needed to calculate the rate constants of the cIST processes, Eq. (3), were reported in the two preceding studies and, here, they have been re-analyzed in a more detailed way. More specifically, final electronic states of the dimer [denoted by index β in Eq. (3)] have been considered explicitly for each collision trajectory and their relative

abundances have been calculated for each particular value of the impact-parameter (and for each initial electronic state, α, of the dimer ion). If we denote these abundances as $x_{\alpha\beta}(b)$, then the effective cross-sections of processes given by Eq. (3) can be calculated from

$$\sigma^{(3)}_{\alpha\beta} = \int_0^{b_{\max}} x_{\alpha\beta}(b)\ 2\pi b\ \mathrm{d}b. \tag{7}$$

Corresponding rate constants have then been obtained from these cross-sections (and momentum-transfer cross-sections of $Kr_2^+(\alpha)$/Kr collisions reported in Refs. 19 and 20) via a series of Monte Carlo simulations [26] described in detail, e.g., in Sec. 2.3 of Ref. 19. Briefly, a sufficiently large number of trajectories of the dimer ion (prepared in a specific electronic state and propagated under the action of a uniform electric field) are generated with collisions evoked with probabilities given by the pre-calculated effective cross-sections. Since weakly ionized gas is assumed, only collisions with neutral atoms are considered [27]. The propagation of each ion takes place until the latter disappears (dissociates) and/or time limits indicating that the cathode has been reached or the prefixed simulation time has been elapsed are exceeded. The reaction rate constant of a particular cIST process is then obtained from (see, e.g., Sec. 2.3 of Ref. 19)

$$k^{(3)}_{\alpha\beta} = \frac{\left\langle \nu^{(3)}_{\alpha\beta} \right\rangle}{N}, \tag{8}$$

where N denotes particle density of the gas and $\left\langle \nu^{(3)}_{\alpha\beta} \right\rangle$ is the average frequency of collisions leading to an $\alpha \to \beta$ transition in the colliding dimer ion.

2. Rate constants of spontaneous radiative processes

The processes resulting from radiative transitions in the Kr_2^+ ion basically consist of two steps. Firstly, an electronic transition takes place (accompanied by the emission of a photon) and, secondly, the dimer either survives or dissociates depending on whether the transition yields a bound rotational-vibrational state or a continuum state. **Alike for collision-induced processes, the effect of the external electric field is completely negligible and it need not be considered for radiative processes. Moreover, since** the electronic transition is much slower than the following dissociation of the dimer (if any), the rate of the overall process is completely governed by the rate of the former process.

The rate constant of a radiative transition going from state α to state β ($\Gamma_{\alpha\beta}$) is given, for a particular nuclear configuration ($\mathbf{R}$), from Fermi's golden rule [28],

$$\Gamma_{\alpha\beta}(\mathbf{R}) = \frac{1}{3\pi\varepsilon_0\hbar^4c^3}\left[E_\alpha(\mathbf{R}) - E_\beta(\mathbf{R})\right]^3\left|\mu_{\alpha\beta}(\mathbf{R})\right|^2, \tag{9}$$

where ε_0, $\hbar$, and c are the vacuum permittivity, the (reduced) Planck constant, and the vacuum light velocity, respectively, E_α and E_β are (adiabatic) electronic energies before and after the transition, respectively, and $\mu_{\alpha\beta}$ is the transition dipole moment between states α and β, both evaluated in nuclear geometry $\mathbf{R}$. For flexible molecules, the values obtained from Eq. (9) have to be averaged over a representative set of molecular geometries. In the case of the Kr_2^+ dimer, it means that averaging over properly sampled inter-atomic distances has to be done. For example, sampling from (the square of) the nuclear wave function corresponding to a specific rotational-vibrational state of the dimer ($[j = 0, v = 0]$ in this work) can be used.

Only specific spontaneous radiative transitions are allowed in the krypton dimer ion if a first-order (dipole) approximation adopted in Eq. (9) is used:

$$\begin{aligned}
&\mathrm{II}(1/2)_\mathrm{g} \rightarrow \mathrm{II}(1/2)_\mathrm{u} \quad [\alpha = 6 \rightarrow \beta = 5],\\
&\mathrm{II}(1/2)_\mathrm{g} \rightarrow \mathrm{I}(1/2)_\mathrm{u} \quad [\alpha = 6 \rightarrow \beta = 1],\\
&\mathrm{I}(3/2)_\mathrm{u} \rightarrow \mathrm{I}(3/2)_\mathrm{g} \quad [\alpha = 3 \rightarrow \beta = 2],
\end{aligned} \tag{10}$$

$$\mathrm{I}(1/2)_\mathrm{g} \rightarrow \mathrm{I}(1/2)_\mathrm{u} \quad [\alpha = 4 \rightarrow \beta = 1], \tag{11}$$

and

$$\mathrm{II}(1/2)_\mathrm{u} \rightarrow \mathrm{I}(1/2)_\mathrm{g} \quad [\alpha = 5 \rightarrow \beta = 4]. \tag{12}$$

Since the transitions given by Eq. (10) end up in a bound (though often excited) rotational-vibrational state on the final electronic potential energy curve, they are hereafter treated as rIST processes of Eq. (5). The transition given by Eq. (12), on the other hand, ends always in a continuum state of the $\mathrm{I}(1/2)_\mathrm{g}$ potential and is thus treated as an rDD process given by Eq. (6). Finally, the process given by Eq. (11) should mostly lead to a bound electronically ground-state dimer, but in an extremely highly excited rotational-vibrational state, lying just below the dissociation limit. For this reason, the process of Eq. (11) is assumed to be an rDD [Eq. (6)]. As a consequence, the rate constants of the spontaneous emission processes have been set as follows (brackets indicate averaging over Kr_2^+ inter-nuclear distances): $k_{65}^{(5)} = \langle\Gamma_{65}\rangle$, $k_{61}^{(5)} = \langle\Gamma_{61}\rangle$, $k_{32}^{(5)} = \langle\Gamma_{32}\rangle$, $k_4^{(6)} = \langle\Gamma_{41}\rangle$, and $k_5^{(6)} = \langle\Gamma_{54}\rangle$. The remaining radiative rate constants are equal to zero.

C. Modeling of kinetics of Kr_2^+ inter-state transitions and decay

Though Eqs. (3)–(6) do not represent a complete description of processes one can anticipate in cold krypton plasma, e.g., reactions leading to the formation of the Kr_2^+ ion are not included, they may provide a qualitatively sound picture of how initial electronic excitations are relaxed in a population of Kr_2^+ ions. Corresponding time evolution is governed by the following kinetic equations [n_α denotes the particle density of the $Kr_2^+(\alpha)$ ion]:

$$\frac{\mathrm{d}n_\alpha}{\mathrm{d}t} = -K_\alpha n_\alpha + \sum_{\beta\neq\alpha} K_{\beta\alpha} n_\beta, \tag{13}$$

where

$$\begin{aligned} K_\alpha &= \left[\sum_{\beta\neq\alpha} k_{\alpha\beta}^{(3)} + k_\alpha^{(4)}\right] n_\mathrm{g} + \sum_{\beta\neq\alpha} k_{\alpha\beta}^{(5)} + k_\alpha^{(6)}, \\ K_{\beta\alpha} &= k_{\beta\alpha}^{(3)} n_\mathrm{g} + k_{\beta\alpha}^{(5)}. \end{aligned} \tag{14}$$

In Eqs. (14), n_g denotes the particle density of the carrier gas. This density is considered constant and is obtained from the gas pressure (P) and temperature (T) calculated within the ideal-gas approximation, $n_\mathrm{g} = P/(k_\mathrm{B}T)$.

Eq. (13) can be rewritten in a compact matrix form,

$$\frac{\mathrm{d}\mathbf{n}}{\mathrm{d}t} = \mathbf{A}\cdot\mathbf{n}, \tag{15}$$

where $\mathbf{n}$ is a six dimensional column vector of $Kr_2^+(\alpha)$ concentrations, $\mathbf{A}$ is a 6×6 matrix corresponding to the constant coefficients of the right-hand side of Eq. (13), and the dot denotes matrix multiplication. Using this compact form of the kinetics equations, their (unique) solution corresponding to an initial condition $\mathbf{n}(0) = \mathbf{n}_0$ can be expressed as

$$\mathbf{n}(t) = \exp(\mathbf{A}t)\cdot\mathbf{n}_0. \tag{16}$$

A symplectic integrator based on a second-order approximation of the matrix exponential, $\exp(\mathbf{A}\Delta t) \approx \mathbf{1} + \mathbf{A}\Delta t + 1/2(\mathbf{A}\Delta t)^2$, has been employed to evaluate this solution numerically.

III. RESULTS AND DISCUSSIONS

A. Reaction rate constants

1. Dimer ion disappearance rate constants

As mentioned above, the *collision-induced dimer ion disappearance* (cDID) rate constants were reported for the Kr_2^+ ion in two immediately preceding studies [19, 20] and the reader is referred therein for necessary details. For completeness, they are also summarized in a form appropriate for the present analysis [29] in Fig. 2.

Rate constants of *radiative dimer dissociation* (rDD) processes [Eqs. (11) and (12)] calculated in this work are also added in Fig. 2 for comparison. However, since the rDD rate constants are, at ambient conditions ($T = 300\,\mathrm{K}$ and $P = 760\,\mathrm{Torr}$), about 2–4 orders of magnitudes smaller than respective cDID rate constants (see also Table I), it seems that the radiative dissociation of the electronically excited Kr_2^+ ions plays only a negligible role at room temperature and atmospheric pressure. Interestingly, this holds even if weak external fields (resulting in low Kr_2^+/Kr collision energies) are considered.

2. Inter-state transition rate constants

The inter-state transition rate constants, as calculated for rotationally-vibrationally ground-state Kr_2^+ dimers, are summarized in Fig. 3. Both collision-induced inter-state transitions (cIST) as well as radiative transitions (rIST) are considered (for the latter see also Table I). A couple of important observations are clear from the figure.

Firstly, the radiative (rIST) processes are either significantly less efficient than the collision-induced (cIST) processes or, at the utmost, comparable to them. But, the latter holds only when collision-induced transitions themselves are unimportant. It thus seems that the radiative transitions will play a negligible role for inter-state transitions [30] as well as for the dimer disappearance.

Secondly, the rate constants of transitions from group I to group II are either zero or by at least two orders of magnitude smaller than the rate constants of transitions occurring among states of group I. The group I to group II transitions are thus expected to play only a marginal role and, as expected [20], the electronic relaxation of group I states is almost

quasiadiabatic, i.e., confined to the group I manifold.

Thirdly, the situation is somewhat more involved for intergroup transitions. While the transitions starting from the $\mathrm{II}(1/2)_\mathrm{g}$ state dominantly go to the $\mathrm{II}(1/2)_\mathrm{u}$ state, i.e., they are confined within group II and are, thus, quasiadiabatic, the lower of the group II states, $\mathrm{II}(1/2)_\mathrm{u}$, may undergo collision-induced transitions to both the other state of group II, $\mathrm{II}(1/2)_\mathrm{g}$, and the states of group I (mainly the ground state). This particularly holds if a weak electric field is applied ($E/N \lesssim 30\,\mathrm{Td}$) where the two kinds of transitions are of a more or less equal probability. As a consequence, the $\mathrm{II}(1/2)_\mathrm{u}$ state will eventually relax to the electronic ground state of the Kr_2^+ ion and this relaxation, if combined with a quite efficient transition form $\mathrm{II}(1/2)_\mathrm{g}$ to $\mathrm{II}(1/2)_\mathrm{u}$, may thus lead to an observable depletion of the group II states in experimental Kr_2^+ populations. We will return to this interesting point once more in the following subsection.

B. Model evolutions of electronic excitations in Kr_2^+

To analyze the processes leading to the relaxation of initial electronic excitations in the Kr_2^+ ion in a more illustrative way, we present, in this subsection, a series of model time evolutions of occupations of electronic states in Kr_2^+ starting from specific electronic states. The evolutions have been calculated using rate constants obtained for $T = 300\,\mathrm{K}$ and for the carrier gas density corresponding to $P = 760\,\mathrm{Torr}$. The methodology described in Subsec. II C has been used with both spontaneous radiative and collision-induced processes considered, though the former, as discussed above, contribute only marginally.

The results of performed calculations are summarized in Figs. 4–6 in which three representative values of the reduced electric field are considered, a low one ($E/N = 5\,\mathrm{Td}$) representing the $E/N \to 0$ (thermal) limit and other two ($E/N = 300\,\mathrm{Td}$ $E/N = 1000\,\mathrm{Td}$) representing stronger electric fields (higher collision energies) where dimer ion disappearance processes become gradually important.

1. Weak-field region

Selected Kr_2^+ electronic relaxation evolutions predicted for $E/N = 5\,\mathrm{Td}$ are depicted in Fig. 4. As expected from the observations discussed in the preceding subsection, already a first glance at the recorded time profiles reveals quite distinct features seen for processes started from group I electronic states and those started from group II states.

For the ground state, $\mathrm{I}(1/2)_\mathrm{u}$, no visible evolution has been recorded on the time scale considered. Since the transitions to higher electronic states are completely negligible and the same holds for the ion disappearance rate, the initially populated ground state does not change along the whole recorded evolution and also no visible decrease of the dimer abundance is seen.

For the other group I states, a different picture is seen since a) the electronically excited dimer ions may disappear (dissociate) much easily than the ground state due to a considerably reduced binding energy and b) downward collision-induced electronic transitions are quite efficient even in the $E/N \to 0$ limit (see Fig. 3). A common feature observed for all the initial electronic excitations belonging to group I is that the Kr_2^+ ion always relaxes, quite fast ($t \leq 10^{-3}\,\mu\mathrm{s}$), to the electronic ground state (with intermediate, lower lying electronic states always involved).

The evolutions recorded for group II states are mainly governed by the dimer ion disappearance which leads to a quite considerable decrease of the dimer abundance. However, the conversion of the initial electronic excitation to the electronic ground state is also observed in survived dimers, either directly if the evolution starts from the $\mathrm{II}(1/2)_\mathrm{u}$ state, or indirectly through the $\mathrm{II}(1/2)_\mathrm{u}$ states if the evolution starts from the $\mathrm{II}(1/2)_\mathrm{g}$ state. Noteworthy, intermediate group I states are skipped (their normalized abundances are well below 10^{-4}). The non-zero value of the rate constant of the $\mathrm{II}(1/2)_\mathrm{u} \to \mathrm{I}(1/2)_\mathrm{u}$ transition is clearly responsible for the observed group II to group I conversion and, thus, the break of the quasiadiabaticity of the underlying processes. Since, on the other hand, the value of this rate constant is much smaller than the value of the rate constant of the $\mathrm{II}(1/2)_\mathrm{g} \to \mathrm{II}(1/2)_\mathrm{u}$ transition, the evolution still remains quasiadiabatic at short time-scales (up to about $t \approx 10^{-3}\,\mu\mathrm{s}$) and the quasiadiabaticity is thus violated only at times about an order of magnitudes longer ($t \geq 10^{-2}\,\mu\mathrm{s}$).

2. Strong-field region

In the case of a strong external electric field, a somewhat different picture is seen **(see Figs. 5 and 6)**, mainly because the efficiency of the collision-induced dimer ion disappearance becomes, even for the most bound $I(1/2)_u$ and $I(3/2)_g$ states, gradually enhanced.

While, for the initial electronic excitations belonging to group I, their subsequent relaxation roughly follows the patterns observed at weak electric fields, two major differences are observed. Firstly, the role of intermediate, lower-lying states **is gradually reduced as** E/N **increases**, and, secondly, the dimer ion disappearance is efficient enough to completely sweep out the initial population of dimers within a fairly short time. As a consequence, it seems that, in stronger electric fields, two main processes compete when group I electronic excitations are relaxed: a) a direct (and fast) conversion of the initial electronic excited state to the electronic ground state and a subsequent (somewhat slower) decay of the ground-state dimer, and b) a direct decay of the excited dimer. The latter mechanism seems to be the more efficient, the higher is the initial excitation.

The situation further simplifies if the initial electronic excitation concerns the group II states. In this case, the role of intermediate electronic states is heavily suppressed and the dimer ion disappearance completely dominates. Noteworthy, however, the traces of the Kr_2^+ ions that survive up to long times almost exclusively populate the electronic ground state.

3. Relevance of Kr_2^+ *excited electronic states*

To estimate the effect of particular electronic excitations of Kr_2^+ on the transport and other macroscopic properties of the dimer ions in krypton gas, we have estimated the number of collisions the dimer ions undergo with krypton atoms before they change their electronic state and/or disappear (dissociate). In general, one may suppose that the effect will be the more pronounced, the larger is the number of such collisions.

In weak electric fields, all the initial electronic excitations are eventually converted in the Kr_2^+ ion to the electronic ground state, $I(1/2)_u$, unless the ion disappears (dissociates). However, while a typical relaxation time is below $t \approx 10^{-3}\,\mu$s for the initial Kr_2^+ electronic excitations belonging to group I, it increases considerably if group II excitations are involved

(up to $t \approx 10^{-2} - 10^{-1}\,\mu$s). It means that group II excitations may survive quite long in Kr_2^+ ions for the excited ions to undergo a significant number of collisions with carrier gas atoms and to contribute to observed macroscopic features (e.g., transport properties) of experimental Kr_2^+ populations.

More specifically, the total mean collision frequency of Kr_2^+/Kr collisions is estimated, at ambient conditions and for $E/N = 5\,$Td, to about $\nu_{\mathrm{coll}} \approx 10^5\,\mu\mathrm{s}^{-1}$. Then, a Kr_2^+ ion initially excited to the $\mathrm{II}(1/2)_\mathrm{u}$ state, which is expected to survive for $t \approx 10^{-2} - 10^{-1}\,\mu$s, should undergo about $10^3 - 10^4$ collisions with neighboring Kr atoms. A dimer ion created in the $\mathrm{II}(1/2)_\mathrm{g}$ state, on the other hand, is expected to undergo much less Kr_2^+/Kr collisions (dozens, a comparable number one gets for the group I electronic excitations) since its life time is much shorter (about $t \approx 10^{-4} - 10^{-3}\,\mu$s). However, a non-negligible amount of Kr_2^+ ions occupying the $\mathrm{II}(1/2)_\mathrm{u}$ state results from ions initially excited to the $\mathrm{II}(1/2)_\mathrm{g}$ state and these $\mathrm{II}(1/2)_\mathrm{u}$ ions participate, afterwards, in thousands of collisions before they dissociate and/or relax to the electronic ground state. As a consequence, ion dimers electronically excited to the group II states, the $\mathrm{II}(1/2)_\mathrm{u}$ state in particular, are expected to play a role in weak electric fields and should be considered in the analysis and interpretation of experimental data.

In the strong field region, a very fast depletion of the initial population of Kr_2^+ is observed for both the electronic ground-state dimer as well as initially electronically excited dimers, typical disappearance times being about $t \approx 10^{-3}\,\mu$s for the ground state and $t \approx 10^{-4}\,\mu$s for excited states. As a consequence, molecular Kr_2^+ ions are expected to play only a limited role in cold krypton plasmas if strong electric fields are applied. However, since, e.g., for $E/N = 1000\,$Td, the total mean collision frequency is estimated to $\nu_{\mathrm{coll}} \approx 10^6\,\mu\mathrm{s}^{-1}$, the decaying dimer ions may still undergo about several dozens (electronically excited) to several hundreds (ground-state dimer ions) of collisions before they disappear. Since the life time of the ions in their electronic ground state is estimated to be only about an order of magnitude longer than those obtained for electronically excited ions, some effect of the latter cannot be excluded, but will probably not be much important. **Naturally, the recombination processes of Eqs.** (1) **and** (2) **may influence the final picture. However, in the strong field region, they are expected to be much less important than in weak electric fields and, consequently, only a slight effect is presumed from them. Unfortunately, no data are presently available on the recombination rates to make any quantitative**

assessment.

IV. SUMMARY AND CONCLUSIONS

Outputs of preceding dynamical calculations on Kr_2^+/Kr collisions occurring in cold krypton plasma [19, 20] have been re-analyzed to get effective cross-sections and rate constants of collision-induced inter-state transitions in Kr_2^+ ions. In addition, rate constants of inter-state transitions resulting from spontaneous radiative processes occurring in electronically excited Kr_2^+ ions have also been calculated using a semiclassical approach based on the classical treatment of nuclei and a full quantum description of electrons. All the relevant low-lying electronic states of the Kr_2^+ ion have been taken into account, namely the $I(1/2)_u$ ground state, excited states asymptotically correlating to the fine-structure ground state ($^2P_{3/2}$) of the atomic ion, $I(3/2)_g$, $I(3/2)_u$ and $I(1/2)_g$ (group I states), and excited states asymptotically correlating to the Kr^+ fine-structure excited state ($^2P_{1/2}$), $II(1/2)_u$ and $II(1/2)_g$ (group II states). For simplicity and practicability of presented calculations, only rotationally-vibrationally ground states of the Kr_2^+ ion have been considered on respective potential energy curves.

The calculated rate constants have subsequently been used in kinetic modelings of electronic relaxation processes in Kr_2^+ ions, initially prepared in a specific electronic state, and their decay. All the modelings have been performed at ambient conditions ($T = 300\,\mathrm{K}$ and $P = 760\,\mathrm{Torr}$) and two representative external electric fields, $E/N = 5\,\mathrm{Td}$ representing the weak-field (thermal) limit and $E/N = 1000\,\mathrm{Td}$ representing the strong-field (high collision energy) limit. It is noteworthy that the radiative processes are much less efficient under these conditions than the non-radiative, collision-induced ones and that a considerable dilution of the carrier gas (by 2 to 6 orders of magnitude, in dependence on the particular transition) would be required to make the radiative processes competitive.

For the weak-field region, it has been found that all the possible initial Kr_2^+ electronic excitations eventually relax to the dimer electronic ground state. This relaxation is faster for group I excitations ($t \approx 10^{-3}\,\mu\mathrm{s}$) than for group II excitations ($t \approx 10^{-2} - 10^{-1}\,\mu\mathrm{s}$). In particular for the group II excitations, the electronic relaxation seems to be slow enough so that the excited dimer ions may influence macroscopic properties of cold krypton plasmas recorded in weak electric fields. It should be also noted, however, that the dimer disappear-

ance (dissociation) becomes increasingly important as the electronic excitation increases. For example, for the group II excitations, the dimer ions that survive up to $t = 1\,\mu$s represent only 20 % of their initial population for the $\mathrm{II}(1/2)_\mathrm{u}$ initial state or even only 5 % for the $\mathrm{II}(1/2)_\mathrm{g}$ initial excitation. Interestingly, the electronic relaxation starting in group II skips group I intermediate states and is relaxed to the dimer ground state either via a direct, $\mathrm{II}(1/2)_\mathrm{u}\rightarrow\mathrm{I}(1/2)_\mathrm{u}$ transition for the $\mathrm{II}(1/2)_\mathrm{u}$ initial excitation or via a bit more involved pathway, $\mathrm{II}(1/2)_\mathrm{g}\rightarrow\mathrm{II}(1/2)_\mathrm{u}\rightarrow\mathrm{I}(1/2)_\mathrm{u}$, if the relaxation starts from $\mathrm{II}(1/2)_\mathrm{g}$.

In the strong-field region, the processes governing the evolution of electronically excited Kr_2^+ are completely dominated by a quite fast decay of the dimers. While the decay of electronically ground-state dimer ions is somewhat slower ($t \approx 10^{-3}\,\mu$s) than the dissociation of electronically excited ions ($t \approx 10^{-4}\,\mu$s), the life times of excited states are almost independent on the particular Kr_2^+ electronic excitation. Like in weak fields, the dimer decay processes include, to some small extent, intermediate electronic states if started from a group I excited state. The group II excitations lead, on the other hand, to a direct dissociation and no intermediate states are observed at a non-negligible abundance.

Preliminary calculations (not reported in this work) seem to indicate that the efficiency of inter-group transitions is considerably reduced if the dimer ion is rotationally-vibrationally excited and, thus, the rotational-vibrational excitations of the dimer will highly probably enhance the role the electronically excited dimers play in cold krypton plasmas. However, a more extensive calculations heavily exceeding the scope of the present work would be needed to provide a reliable assessment of the effect the Kr_2^+ rotational-vibrational excitations have on experimental data.

Last but not least, since processes leading to the formation of krypton dimer ions (e.g., ternary recombination collisions) have not been taken into account in the present work, a complete description of the formation and quenching of electronic excitations in the Kr_2^+ ion in cold krypton plasmas has still not been achieved. Among others, it means that the present data do not allow, by themselves, to estimate the abundances of Kr_2^+ electronic states in cold krypton plasmas and are, thus, not sufficient to resolve the question about the role of electronically excited dimer ions in these plasmas as raised in a preceding publication [20]. Presently, additional calculations focused on the formation of the Kr_2^+ ions are being prepared in our group. Beyond that, however, the present work on the rate constants of processes involving different Kr_2^+ electronic states can be directly used in, for instance, the

electrodynamics modeling of low temperature plasma jets in krypton gas where the plasma active species are governed by the directed streamer development having both a low field region (a few Td) in the streamer channel and a strong field region (a few hundreds of Td) in the streamer head. For this, the rate constants governing the krypton dimer ion populations have been provided and analyzed for both weak-field and strong-field conditions.

Acknowledgments

René Kalus and Cyril Van de Steen express their thanks to the Ministry of Education, Youth and Sports of the Czech Republic for the financial support from the *National Programme of Sustainability* (NPS II) project (grant no. LQ1602) and the *Large Infrastructures for Research, Experimental Development and Innovations* project (grant no. LM2015070), as well as to VSB-TUO (grant no. SP2018/178). Traveling support from the Barrande programme of French-Czech collaboration (grants no. 40688TH and 8J18FR031) is also warmly acknowledged. The calculations have been performed using the resources of the IT4Innovations National Supercomputing Center of the Czech Republic (grant no. OPEN-13-2) and multiprocessing work stations of the parallel computational center of Toulouse.

[1] M. Laroussi, IEEE Trans. Plasma Sci. **37**, 714 (2009).

[2] M. Yousfi, N. Merbahi, A. Pathak, and O. Eichwald, Fund. Clin. Pharm. **28**, 123 (2014).

[3] H. Tanaka, K. Ishikawa, M. Mizuno, S. Toyokuni, M. Kajiyama, F. K. and. H.-R. Metelmann, and M. Hori, Rev. Mod. Plasma Phys. **3**, 1 (2017).

[4] A. I. Bugrova, A. M. Bishaev, A. V. Desyatskov, M. V. Kozintseva, A. S. Lipatov, and M. Dudeck, Int. J. of Aero. Eng. **2013**, ID 686132 (2013).

[5] S. Mazouffre, Plasma Sources Sci. Technol. **25**, 033002 (2016).

[6] H. Helm and M. T. Elford, J. Phys. B **11**, 3939 (1978).

[7] H. Helm, Phys. Rev. A **14**, 680 (1976).

[8] C. Praxmarer, A. Hansel, A. Jordan, H. Kraus, and W. Lindinger, Int. J. Mass Spec. Ion. Proc. **129**, 121 (1993).

[9] T.-K. Ha, P. Rupper, A. Wuest, and F. Merkt, Mol. Phys. **101**, 827 (2003).

[10] R. Kalus, I. Paidarová, D. Hrivňák, P. Paška, and F. X. Gadéa, J. Chem. Phys **294**, 141 (2003).

[11] A. K. Dham, A. R. Allnatt, W. J. Meath, and R. A. Aziz, Mol. Phys. **67**, 1291 (1989).

[12] R. Kalus, Collect. Czech. Chem. Commun. **65**, 141 (2000).

[13] H. Helm, J. Phys. B **9**, 2931 (1976).

[14] M. Tomza, K. Jachymski, R. Gerritsma, A. Negretti, T. Calarco, Z. Idziaszek, and P. S. Julienne, Rev. Mod. Phys **91**, 035001 (2019).

[15] A. D. Dörfler, P. Eberle, D. Koner, M. Tomza, M. Meuwly, and S. Willitsch, Rev. Mod. Phys (2019), 1906.12285.

[16] L. Ratschbacher, C. Zipkes, C. Sias, and M. Köhl, Nature Phys **8**, 649 (2012).

[17] J. Joger, H. Fürst, N. Ewald, T. Feldker, M. Tomza, and R. Gerritsma, Phys. Rev. A **96**, 030703 (2017).

[18] R. Saito, S. Haze, M. Sasakawa, R. Nakai, M. Raoult, H. D. Silva, O. Dulieu, and T. Mukaiyama, Phys. Rev. A **95**, 032709 (2017).

[19] C. Van de Steen, M. Benhenni, R. Kalus, R. Ćosić, S. Illésová, F. X. Gadéa, and M. Yousfi, Plasma Sources Sci. Technol. **28**, 035007 (2019).

[20] C. Van de Steen, M. Benhenni, R. Kalus, R. Ćosić, F. X. Gadéa, and M. Yousfi, Plasma Sources Sci. Technol. (2019), https://doi.org/10.1088/1361-6595/ab3a17.

[21] I. Janeček, M. Stachoň, F. X. Gadéa, and R. Kalus, Phys. Chem. Chem. Phys. **19**, 25423 (2017).

[22] As discussed elsewhere [21], radiative processes do not play an important role during the collision compared to non-radiative processes and are thus neglected here. Moreover, since under ambient conditions the time during which the dimer ion undergoes collisions is much shorter than the time it spends as a free molecule, the effect of radiative processes taking place during the collisions may, in addition, be also considered negligible with respect to the free-flight phase. The probability of free-flight non-radiative transitions in the Kr_2^+ ion is, on the other hand, zero if the spin-orbit coupling is neglected and is almost zero if the spin-orbit coupling is included via the atoms-in-molecules scheme (as done in the present work). As a consequence, the non-radiative free-flight transitions in the Kr_2^+ ion are neither considered in the present work.

[23] Mostly, the dimer disappearance means that the collisionally excited dimer disscociates, $Kr_2^+ + Kr \rightarrow Kr^+ + 2Kr$. However, as discussed in detail in Ref. [20], the dimer-to-monomer charge transfer, $Kr_2^+ + Kr \rightarrow Kr^+ + Kr_2$, leading to the same ionic fragment as the dimer dissociation, may also play a role if specific electronic states of the dimer ion are populated prior to collision. the dimer disappearance channel is thus introduced to represent both reaction mechanisms leading to the monomer ion product without explicitly discriminating between them.

[24] In this work, we use the following numerical labels to specify the electronic state of the ionic dimer: $\alpha = 1$ for $I(1/2)_u$, $\alpha = 2$ for $I(3/2)_g$, $\alpha = 3$ for $I(3/2)_u$, $\alpha = 4$ for $I(1/2)_g$, $\alpha = 5$ for $II(1/2)_u$, and $\alpha = 6$ for $II(1/2)_g$.

[25] In general (see, e.g., Ref. 19), distances in the dimer are sampled from (squares of) nuclear wave functions obtained for a given rotational-vibrational state (ground state in this work) by numerically solving two-particle Schrödinger equation for the two krypton nuclei. Afterwards, nuclear velocities are added in the perpendicular direction to the dimer bond axis to get required rotational angular momentum (does not apply in this work) and along the bond axis to get the required rotational-vibrational energy (zero-point vibration energy in this work).

[26] M. Yousfi, A. Hennad, and O. Eichwald, J. of Appl. Phys. **84**, 107 (1998).

[27] In weakly ionized gas, the ionization degree of about 10^{-6} to 10^{-5} is presumed. It is thus clear that the concentration of electrons is necessarily much lower (by 5 to 6 orders of magnitude) than the concentration of the background gas. Despite the fact that the electron-dimer dissociative recombination has much higher frequency than the dimer-atom collisions (by 1 to 3 order of magnitudes), the effect of dimer collisions with background gas atoms completely prevails over collisions with free electrons.

[28] E. Fermi, *Nuclear Physics* (The University of Chicago Press, Chicago, 1950).

[29] All the (binary) collision-induced processes are considered, in this work, as first-order ones since the particle density of the carrier gas, n_g, enters the kinetic equations as a (presumably constant) parameter. Since related rate constants are multiplied by this constant carrier-gas density in Eqs. (14), they are presented in this multiplied form throughout this paper. The radiative rate constants, on the other hand, enter Eqs. (14) as they are and will thus be presented in the same way (i.e., not multiplied by n_g).

[30] Below in the kinetic modeling part of this section (Subsec. III B), the radiative processes have always been considered. However, no visible changes in calculated time evolutions have been

observed after the radiative rate constants were set to zero.

Figures and Tables

TABLE I: Rate constants (k) and half-times ($\tau = \ln 2/k$) of radiative transitions in the rotationally-vibrationally ground-state Kr_2^+ ion, $[j = 0, v = 0]$, as given by Eqs. (10)–(12).

transition	k [μs^{-1}]	τ [μs]
$II(1/2)_g \rightarrow II(1/2)_u$	0.0009	790
$II(1/2)_g \rightarrow I(1/2)_u$	0.0949	7.3
$I(3/2)_u \rightarrow I(3/2)_g$	0.0050	138
$I(1/2)_g \rightarrow I(1/2)_u$	0.0006	1137
$II(1/2)_u \rightarrow I(1/2)_g$	0.4347	1.6

FIG. 1: Potential energy curves of the lowest-lying electronic states of the Kr_2^+ ion (taken and adapted from Ref. [20]).

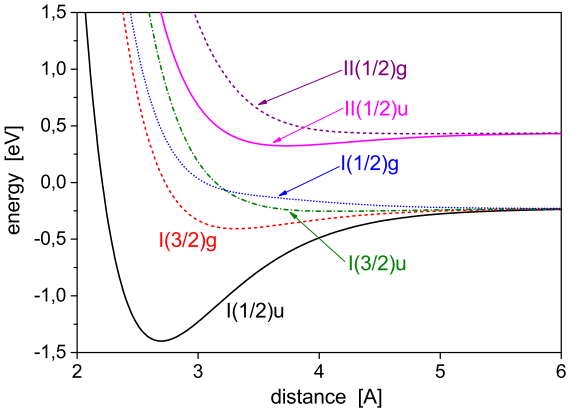


FIG. 2: Normalized rate constants of collision-induced dimer ion disappearance, $n_g k_\alpha^{(4)}$, calculated for rotationally-vibrationally ground-state Kr_2^+ dimers, $[j = 0, v = 0]$, in respective electronic states (group I – open symbols, group II – full symbols) and at room temperature ($T = 300\,\mathrm{K}$). Note that the rate constants are multiplied (see Subsec. II C) by the carrier-gas particle density corresponding to the atmospheric pressure ($P = 760\,\mathrm{Torr}$) and room temperature. For comparison, rate constants of spontaneous radiative dissociation of the Kr_2^+ ion (not multiplied by the gas density) are also provided as horizontal lines framed with respective symbols.

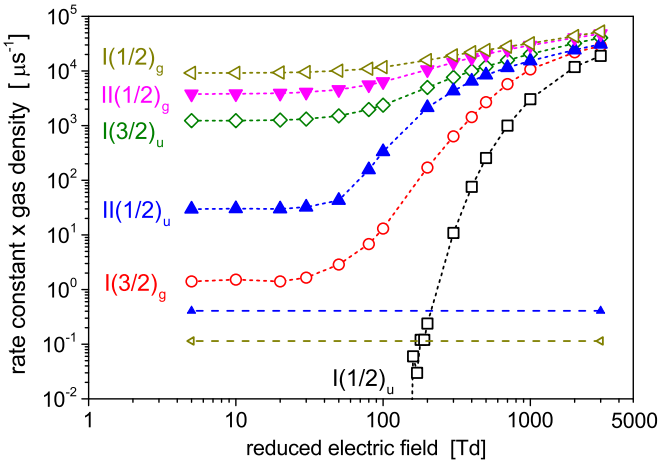


FIG. 3: Normalized rate constants of collision-induced inter-state transitions, $n_g k^{(3)}_{\alpha\beta}$, calculated for rotationally-vibrationally ground-state Kr_2^+ dimers, $[j = 0, v = 0]$, initially created in electronic states indicated in respective panels and for room temperature ($T = 300\,\mathrm{K}$). Like in Fig. 2, the rate constants are multiplied by the carrier-gas particle density set to the value corresponding to $P = 760\,\mathrm{Torr}$ and room temperature. Rate constants of inter-state transitions due to spontaneous radiative processes in Kr_2^+ (not multiplied by the gas density) are also provided as dashed horizontal lines framed with respective symbols. If a particular curve is missing in any panel, the corresponding rate constant is equal to zero for all the values of the reduced electric field considered.

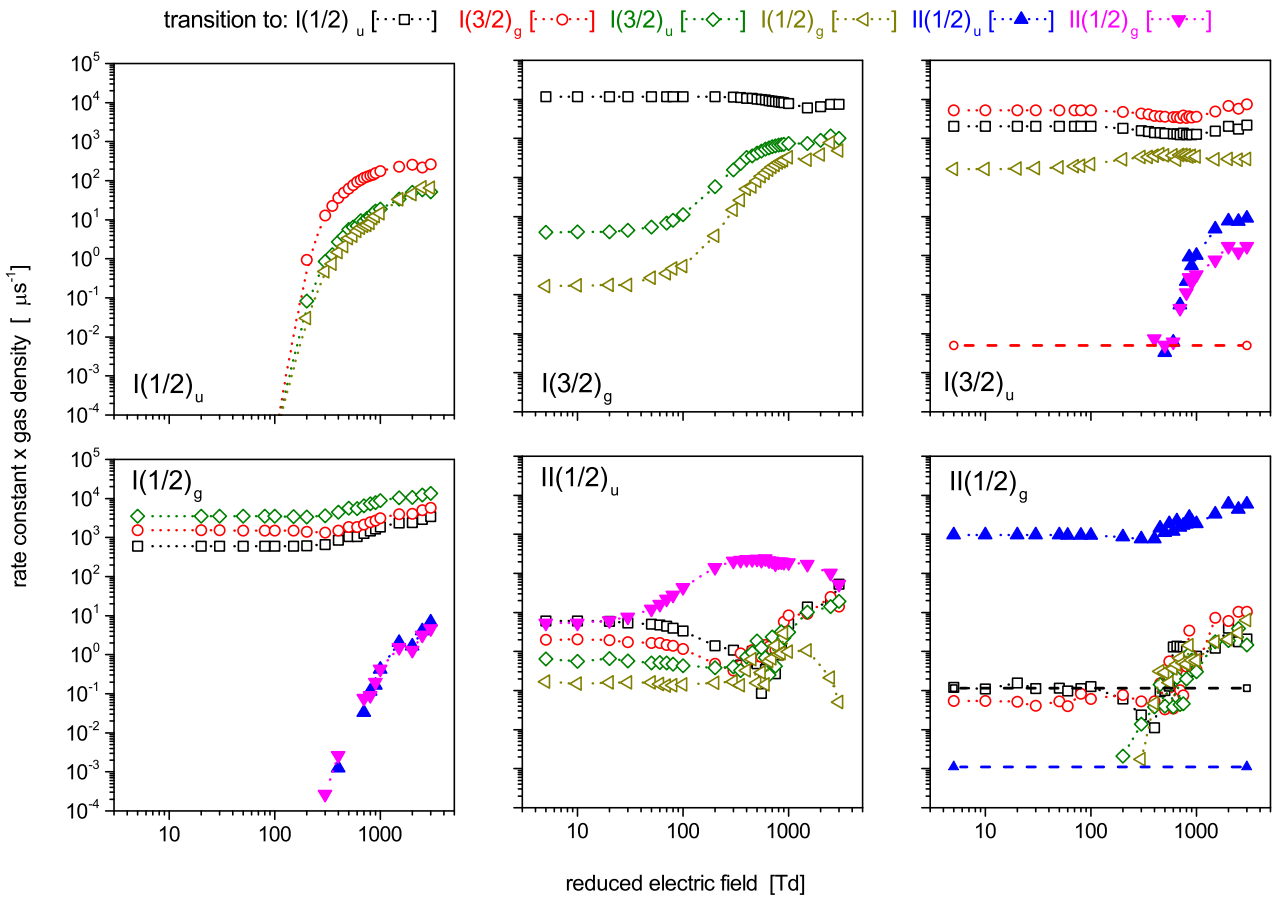


FIG. 4: Time evolutions of normalized abundances of Kr_2^+ electronic states [$n_\alpha(t)/n_0$, where n_0 is the total Kr_2^+ density at $t = 0$] in populations of ionic dimers initially populating a particular electronic state (indicated on the right of each panel) as calculated for $E/N = 5\,\mathrm{Td}$. Note that the processes leading to the creation of the Kr_2^+ dimer [Eqs. (1) and (2)] are not considered in this figure. For this reason, time evolutions of $n(t)/n_0$ [$n(t) = \sum_\alpha n_\alpha(t)$] are also shown (thick gray lines) to visualize the progress of the dimer ion disappearance. Note also that the rotational-vibrational ground state is assumed to be unchanged in Kr_2^+ for all the considered times.

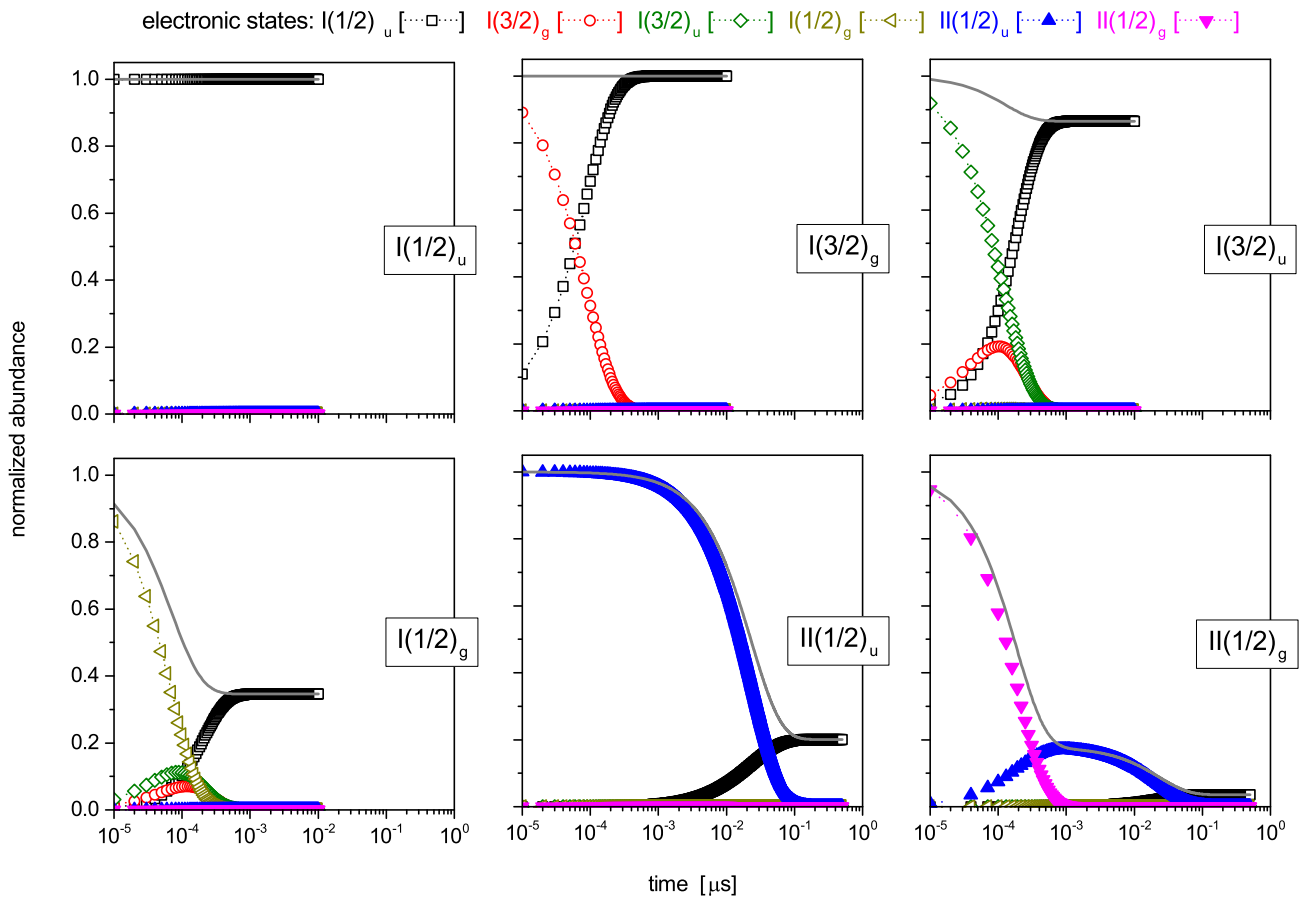


FIG. 5: The same as in Fig. 4, but calculated for $E/N = 300\,\mathrm{Td}$.

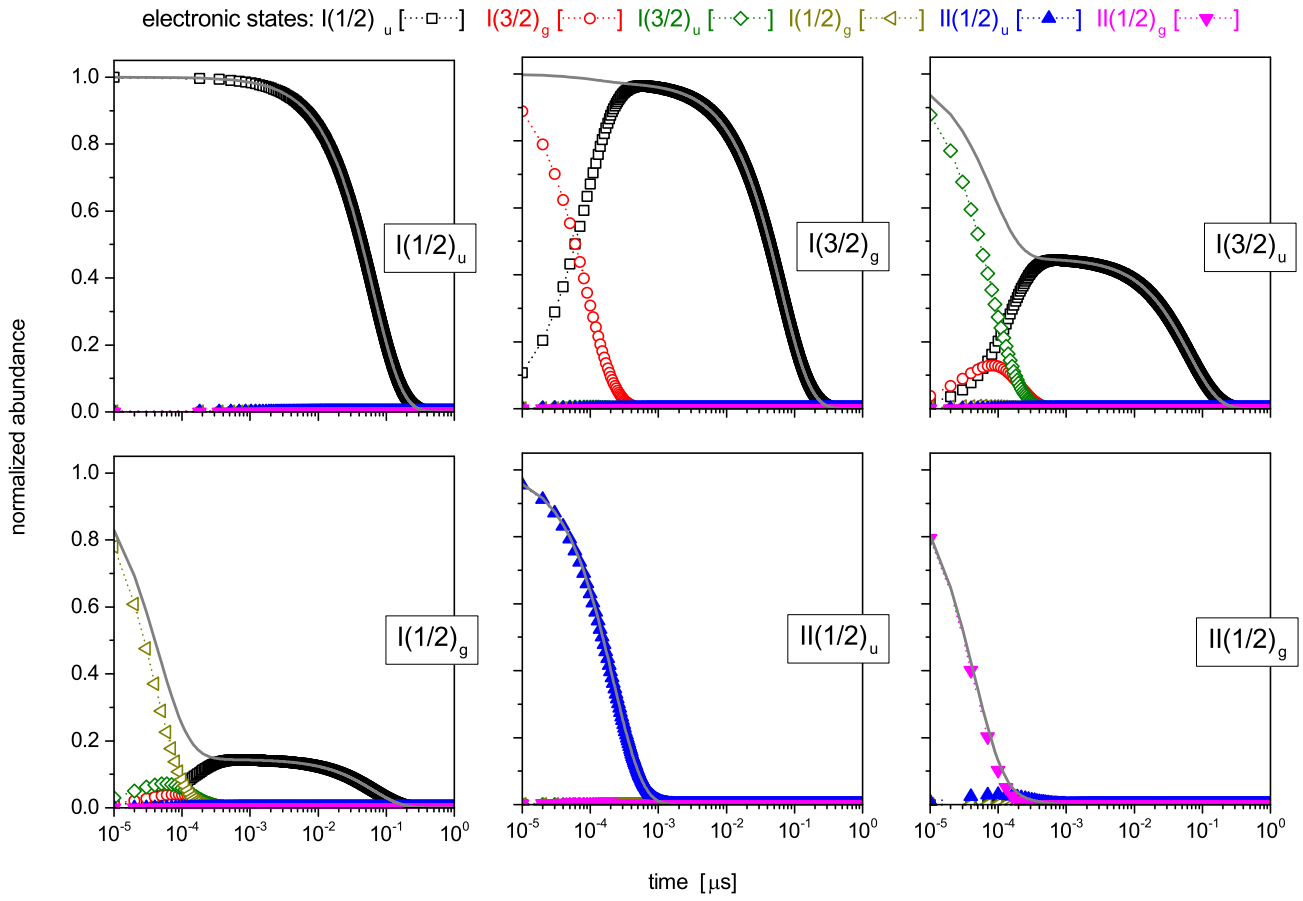


FIG. 6: The same as in Fig. 4, but calculated for $E/N = 1000\,\mathrm{Td}$. **(Note that a different time scale is used in this figure.)**

